Technically Complete, March 11, 2016

APPENDIX III-D.5-1

SUMMARY OF GEOTECHNICAL DESIGN PARAMETERS

STATE OF TEXAS
JESSE PAUL VARSHO
114074
LICENSED
PROFESSIONAL ENGINEER

9-4-15

This document is released for the purpose of permitting only under the authority of Jesse P. Varsho, P.E. #114074. It is not to be used for bidding or construction. Texas Registered Engineering Firm F-5650

CB&I

CB&I Environmental & Infrastructure	Client Name:	Rancho Viejo Waste Management, LLC		
	Project Name:	Pescadito Environmental Resource Center	Project No.:	148866
	Prepared by:	P. Thomas	Date Prepared:	2/24/2015
	Reviewed by:	Jesse P. Varsho, PE	Date Reviewed:	3/2/2015

TITLE: SUMMARY OF GEOTECHNICAL DESIGN PARAMETERS

Problem Statement

Summarize the geotechnical design parameters for the various landfill and in-situ materials present at the Pescadito Environmental Resource Center Project Site.

References

The referenced literature cited below is provided in the attached pages. Referenced site specific information is provided within the Application as stated below.

1. The site Geology Report (dated 2015) contained in this Application — as it pertains to subsurface investigative data refer to Appendix III-E.1 of the Geology Report.
2. The site Geology Report (dated 2015) contained in this Application — as it pertains to geotechnical test data refer to Appendix III-E.2 of the Geology Report.
3. Design Drawings contained in this Application.
4. Holtz, R.D., and Kovacs, W.D. (1981). “An Introduction to Geotechnical Engineering.” Prentice-Hall, 1981.
5. Duncan, J.M, Wright, S.G., and Brandon, T.L. (2014). “Soil Strength and Slope Stability.” John Wiley and Sons Inc., 2nd Edition, 2014.
6. Terzaghi, K., Peck, R.B., and Mesri, G. (1996). “Soil Mechanics in Engineering Practice.” John Wiley and Sons Inc., 3rd Edition, 1996.
7. Bowles, J.E. (1996). “Foundation Analysis and Design.” McGraw-Hill, 5th Edition, 1996.
8. Nixon, N., and Jones, D.R. (2005). “Engineering Properties of Municipal Solid Waste.” *Journal of Geotextiles and Geomembranes*, 23(2005), 205-233.
9. Zekkos, D., Bray, J.D., Kavazanjian, E., Jr., Matasovic, N., Rathje, E.M., Riemer, M., and Stokoe, K.H., II (2006). “Unit Weight of Municipal Solid Waste.” *Journal of Geotechnical and Geoenvironmental Engineering*, 132(10), 1250-1261.
10. Kavasanjian Jr., E. (2008). “The Impact of Degradation on MSW Shear Strength.” *GeoCongress 2008*, 224-231.
11. Sharma, H.D., and Anirban, D. (2007). “Municipal Solid Waste Landfill Settlement: Postclosure Perspectives.” *Journal of Geotechnical and Geoenvironmental Engineering*, 133(6), 619-629.
12. Bareither, C. (2008). "Compression Indices for Full-Scale Landfills." Compilation of Primary and Secondary Compression Indices from Literature (attached pages).
13. Interface Shear Test Results for various geosynthetic interfaces (attached pages).
14. USGS Seismic Hazard Map of the United States (attached pages).
15. USEPA (1993). “Solid Waste Disposal Facility Criteria Technical Manual.” EPA530-R-93-017, November 1993.

CB&I Environmental & Infrastructure	Client Name:	Rancho Viejo Waste Management, LLC		
	Project Name:	Pescadito Environmental Resource Center	Project No.:	148866
	Prepared by:	P. Thomas	Date Prepared:	2/24/2015
	Reviewed by:	Jesse P. Varsho, PE	Date Reviewed:	3/2/2015
TITLE:	SUMMARY OF GEOTECHNICAL DESIGN PARAMETERS			

Technically Complete, March 11, 2016

Assumptions

The landfill will include the following components as detailed below (**from top to bottom**):

- Final Cover System (4H:1V Slope)
  - 7-inch Vegetative Cover / Erosion Control Layer
  - 30-inch Infiltration Layer
  - 12-inch Intermediate Cover (Intermediate Cover is included as part of the Waste Layer for analysis purposes)
- Waste (maximum waste column thickness of approximately 380 feet occurring through peak final landform elevation of the North and South Unit Landfills)
- Leachate Collection / Liner System on 3H:1V Landfill <u>Sideslopes</u> (**Reference No. 3**)
  - *Protective Soil Layer (2-feet thick)*
  - *Geosynthetics - Option 1*
    - Geotextile Slip Layer
    - Double-Sided Drainage Geocomposite
    - 60-mil Textured HDPE Geomembrane
  - *Geosynthetics - Option 2*
    - Geotextile Slip Layer
    - Double-Sided Drainage Geocomposite
    - Bentonite Enhanced Textured FML (bentonite side faced down)
    - Bentonite Enhanced Textured FML (bentonite side faced up)
  - *Compacted Low Permeable Soil Liner ($k \leq 1x10^{-7}$ cm/sec)*
    - MSW Cells (2-feet thick)
    - Class I Waste Cells (3-feet thick)
- Leachate Collection / Liner System on Landfill <u>Base</u> (**Reference No. 3**)
  - *Protective Soil Layer (2-feet thick)*
  - *Geosynthetics - Option 1*
    - Double-Sided Drainage Geocomposite
    - 60-mil Textured HDPE Geomembrane
  - *Geosynthetics - Option 2*
    - Double-Sided Drainage Geocomposite
    - Bentonite Enhanced Textured FML (bentonite side faced down)
  - *Compacted Low Permeable Soil Liner ($k \leq 1x10^{-7}$ cm/sec)*
    - MSW Cells (2-feet thick)
    - Class I Waste Cells (3-feet thick)

- In-Situ / Foundation Soils
    - *Stratum I* - Stratum I has been reported to consist of clays and sandy clays, with limited presence of sand and occasional gravel and cobbles. The clays have been characterized as having a stiff to firm consistency, and occur at ground surface (*where present*) to a maximum depth of 18-feet below ground surface (ft bgs) (**Reference No. 1**).
    - *Stratum II* - Stratum II has been reported to consist of predominantly clays with minor occurrence of sandy clay and organic (plant root) materials. The clays have been characterized as having a stiff to hard consistency, and occur at ground surface (*where present*) to depths of up to 10-ft bgs with a maximum thickness of 10 feet (**Reference No. 1**).
    - *Stratum III* - Stratum III has been reported to consist of clay and sandy, silty clay with thinly to very thinly interbedded claystone, siltone, and sandstone seams and lenses (i.e., bedding units typically 1 to 2 feet or less). The clays have been characterized as having a hard consistency, and occur at depths ranging from approximately 2- to 39-ft bgs with a unit thickness ranging from approximately 8- to 33-feet (**Reference No. 1**).
    - *Stratum IV* - Stratum IV has been reported to consist predominantly clay and sandy, silty clay, with thinly to very thinly interbedded claystone, siltstone and sanstone seams and lenses (i.e., bedding units 1 to 2 feet or less). The clays have been characterized as having a hard consistency, and occur throughout the site at depths ranging from approximately 16-ft.bgs to greater than 160-ft.bgs with a unit exceeding 144-feet (**Reference No. 1**).

  Note, the Stratum I and II soils are not continuous across the site and occur at very shallow depths below ground surface (*where present*).

Material Properties of Geologic Units

A discussion of the material properties including unit weights, shear strength, and consolidation parameters for the uppermost geologic units occurring at the site are discussed below. Because the Stratum II, III, and IV soils exhibit the same material properties (including but not limited to shear strength) the three soils were combined and modeled in the geotechnical stability calculations as one lithologic unit / soil layer. The Stratum I soils were modeled as a separate soil unit / layer.

Unit Weights and Shear Strength

The in situ moist and saturated unit weights assumed for Stratum I, and the combined Stratum II, III, and IV soils are based on a review of laboratory test data / reports contained in **Reference No. 2** and are summarized on **Table 1** on the following page.

The shear strength parameters of the soils were conservatively estimated based on a review of the following information:

- Field shear strength data (based on pocket pentrometer readings) reported on the soil boring logs in **Reference No. 1**,
- Laboratory tested plasticity indices (**Reference No. 2**) and
- Correlations made between plasticity indices and shear strength values (**Reference Nos. 4**, **5**, and **6**).

CB&I Environmental & Infrastructure	Client Name: Rancho Viejo Waste Management, LLC	
	Project Name: Pescadito Environmental Resource Center	Project No.: 148866
	Prepared by: P. Thomas	Date Prepared: 2/24/2015
	Reviewed by: Jesse P. Varsho, PE	Date Reviewed: 3/2/2015

TITLE: SUMMARY OF GEOTECHNICAL DESIGN PARAMETERS

Based on a review of the logs of borings contained in **Reference No. 1** — the average shear strength was estimated to be approximately 2,250 psf for the Stratum I soils, and approximately 4,500 psf for the Stratum II-III-IV soils.

Based on a review of the laboratory test data contained in **Reference No. 2** — the average plasticity index (PI) was estimated to be approximately 25 for the Stratum I soils, and approximately 35 for the combined Stratum II-III-IV soils. Using empirical correlations contained in **Reference Nos. 4**, **5**, and **6**, the long-term shear strength friction angle for the Stratum I soil is estimated to be between 27 and 30 degrees based on the approximate average PI of 25 that was estimated for the Stratum I soil. Similarly the long-term shear strength friction angle for the Stratum II-III-IV soils was estimated to be between 25 and 28 degrees using the approximate average PI value of 36 that was estimated for the Stratum II-III-IV soils. A summary of these correlated values are presented on **Table 1** below.

Table 1
Material Properties of Site Geologic Units

Layer Description	Moist Unit Weight γ_{moist}	Saturated Unit Weight γ_{sat}	Approximate Average Shear Strength Obtained from Field Pocket Penetrometer Readings	Correlation Between Plasticity Index and Shear Strength [1,2]		Shear Strength Values Conservatively Assumed For Geotechnical Stability Calculations			
						Shear Strength Short-Term Conditions		Shear Strength Long-Term Conditions	
				Approximate Average Plasticity Index	Friction Angle ϕ'	Cohesion c	Friction Angle ϕ	Cohesion c'	Friction Angle ϕ'
Stratum I	125 pcf	126 pcf	2,250 psf	25	27° to 30°	1,000 psf	0°	250 psf	10°
Stratum II-III-IV	129 pcf	132 pcf	4,500 psf	36	25° to 28°	2,500 psf	5°	720 psf	13.5°

Notes
1. Plasticity Indices reported above represent approximate averages based on a review of the laboratory tested Atterberg Limits reported in Reference No. 2.
2. Correlations between Plasticity Index and Shear Strength are based on a review of empirical correlations cited in Reference Nos. 4, 5, and 6.

The shear strength values utilized in the geotechnical stability calculations (reported above in last few columns of **Table 1**) for short-term and long-term conditions were conservatively assumed lower than the values estimated from the field measurements and correlated PI values. Specifically, for the short-term conditions approximately one-half of the field measured undrained shear strength cohesion was assumed with a friction angle of zero for Stratum I and a very small friction angle value of five degrees was assumed for the Stratum II-III-IV soils. For the long-term conditions, low friction angle values were assumed to represent potential “softening” or residual shear strength conditions of the soils, with low values for cohesion.

Consolidation Parameters

The base liner of the North and South Units will be entirely in the Stratum IV soils, with the approximate upper one-third of the sideslope liners in the Stratum III soils, and the approximate lower two-thirds of the sideslope liners in the Stratum IV soils. The consolidation parameters for settlement calculations were therefore only considered for the combined Stratum II-III-IV soil unit / layer. The consolidation parameters (compression index, recompression index, and secondary compression index) were calculated using empirical correlations between the various consolidation parameters and plasticity index. As stated earlier, an average plasticity index of approximately 36 was estimated for the combined Stratum II-III-IV soils (**Reference No. 2**). The consolidation parameters are summarized below in **Table 2**. Based on a review of laboratory test data/reports contained in **Reference No. 2**, an average void ratio (e_o) of approximately 0.64 was estimated and is presented below in Table 2 (later used in the foundation settlement calculations).

Table 2
Geologic Units
Consolidation Parameters

Geologic Unit / Layer	Void Ratio (e_O)	Average Plasticity Index	Compression Index (C_c)	Recompression Index (C_r)	Secondary Compression Index (C_α)
Stratum II-III-IV	0.64	36	0.4204	0.0609	0.0136

Notes:

1. Void ratio of 0.64 represents an estimated approximate average based on laboratory test data (Reference No. 2).
2. Compression Index (C_c) was calculated using the following correlation (Reference No. 7): $C_c = 0.046 + (0.0104 \times PI)$
3. Recompression Index (C_r) was calculated using the following correlation (Reference No. 7): $C_r = 0.00194 \times (PI - 4.6)$
4. Secondary Compression Index (C_α) was calculated using the following correlation (Reference No. 7): $C_\alpha = 0.00168 + (0.00033 \times PI)$

Overconsolidation Ratio

The overconsolidation ratio (OCR) was determined using an empirical correlation that utilizes natural water content (w_N), liquid limit (w_L), and the existing effective overburden pressure (p'_o) to determine the preconsolidation pressure (p'_c). The following empirical correlation was used based on **Reference No. 7**:

$$log_{10}p'_c = 5.97 - 5.32\left({}^{w_N}/_{w_L}\right) - 0.25\, log_{10}p'_o$$

Using an estimated average water content and liquid limit of approximately 17% and 58%, respectively for the Stratum II-III-IV soil unit (**Reference No. 2**), and calculating the overburden pressure at the landfill soil liner depth of 100-ft.bgs and an assumed depth of 50-feet below the liner (150-feet) for potential compressible soils, the preconsolidation pressure (p'_c) is solved for. The existing effective overburden pressure (p'_o) at 100-ft.bgs and 150-ft.bgs is 6,960 psf (333.25 kPa) and 10,440 psf (499.87 KPa), respectively. The preconsolidation pressure (p'_c) at 100-ft.bgs and 150-ft.bgs is 125,847 psf (6,026 kPa) and 114,763 psf (5,495 KPa), respectively.

The OCR is then calculated as follows:

$$OCR = \frac{p'_c}{p'_o}$$

$$at\ 100\ ft.bgs = \frac{125{,}847}{6{,}960} = 18$$

$$at\ 150\ ft.bgs = \frac{114{,}763}{10{,}440} = 11$$

The native soil at liner depth and below is determined to be overconsolidated, since the OCR is greater than 1.0. The maximum effective overburden pressure that will occur on the native soils lying directly beneath the proposed compacted soil liner at the time of the complete build-out of the landfill will occur at the location of the maximum waste column thickness of 380-ft. Using the unit weight of 65 pcf for waste fill (discussed on following page) and the thicknesses and unit weight of the final cover, protective cover, and compacted soil liner (total thickness = 3+2+3= 8-ft, and unit weight = 132 pcf), the effective overburden pressure (p'_{final}) at the time of complete landfill build-out is:

$$p_{final} = (380 ft\ waste \times 65\ pcf) + [(8) ft\ soil\ layers \times (132 - 62.4) pcf] = 25{,}257\ psf$$

The estimated effective overburden pressure of 25,257 psf is significantly lower than the effective preconsolidation pressure (p'_C = 125,847 psf) acting on the native soil at liner depth; and therefore it is assumed that the native soils that will underlie the proposed landfill soil liner will be incompressible for purposes of foundation settlement calculations (**Appendix III-D.5-4**).

Material Properties of the Final Cover System

The landfill final cover will consist of 37-inches of the Stratum II-III-IV soils (as discussed earlier, 7 inches vegetative cover and 30 inches infiltration layer). The final cover is assumed to perform as a water balance cover and therefore will not have a geosynthetic barrier layer. For simplicity, the final cover system soil layers were modeled as one unit in the stability calculations. A summary of the unit weights and shear strength parameters are presented on **Table 3** on the following page.

Table 3 Final Cover Unit Weights and Strength Parameters						
			Shear Strength Short-Term Conditions		Shear Strength Long-Term Conditions	
Layer	Moist Unit Weight γ_{moist}	Saturated Unit Weight γ_{sat}	Cohesion c	Friction Angle ϕ	Cohesion c'	Friction Angle ϕ'
Final Cover	129 pcf	132 pcf	720 psf	13.5°	720 psf	13.5°

Material Properties of Waste

Unit Weight and Shear Strength

The unit weight of the landfill waste varies widely because of differences in waste constituents, state of decomposition, degree of compaction, height of placement, amount of daily cover, etc. The total unit weight of waste has been reported in published technical literature to range from 55 pcf up to 95 pcf. A unit weight of 50 pcf (1,350 lbs/cy) has been reported for various sites permitted in Texas and agrees with published data reported for moderately compacted waste (**Reference No. 8**). Assuming that daily and intermediate soil cover will be applied at a ratio of 20% to 80% waste, a weighted average of the landfill waste / cover is calculated to be approximately 65 pcf using a unit weight of 129 pcf for the soil cover material (based on Stratum II-III-IV soils). The value of 65 pcf agrees with data published for the unit weight of waste with soil cover under typical compactive efforts (**Reference No. 9**).

The shear strength of waste that has been assumed is zero cohesion with a friction angle of 30 degrees. This assumed shear strength is based on the conservative assumption that the landfill will operate with continuous leachate recirculation throughout the landfill useful life (**Reference No. 10**). The assumed unit weights and shear strength parameters for waste are summarized below on **Table 4**.

Table 4 Landfill Waste Fill Unit Weights and Shear Strength Parameters				
			Shear Strength Short-Term & Long-Term Conditions	
Layer	Moist Unit Weight γ_{moist} (pcf)	Saturated Unit Weight γ_{sat} (pcf)	Cohesion c, c'	Friction Angle ϕ, ϕ'
Waste Fill (includes daily and intermediate cover)	65	65	0 psf	30°

Consolidation Parameters for Waste

The consolidation parameters presented on **Table 5** below were used to calculate the waste settlement due to compression at the landfill. These values represent averages based on published data (**Reference Nos. 11** and **12**).

Table 5
Landfill Waste Fill
Consolidation Parameters

Layer	Compression Index C'_c	Secondary Compression Index C'_α
Waste	0.25	0.051

Material Properties of Base and Sideslope Leachate Collection / Liner System

Protective Soil Cover Layer

The protective soil cover layer will consist of 24-inches (2-feet) of the excavated Stratum II-III-IV soils placed over the geosynthetics and immediately below the first lift of waste. The protective cover soil unit weights and shear strength values are based on the values assumed for the combined Stratum II-III-IV soil unit/layer (refer to **Table 1**). A summary of the unit weights and shear strength parameters are summarized below on **Table 6**.

Compacted Low Permeable Soil Liner

The compacted low permeable soil liner will be constructed using excavated Stratum II-III-IV soils. The compacted soil liner unit weights and shear strength values are based on the values assumed for the combined Stratum II-III-IV soil unit/layer (refer to **Table 1**). A summary of the unit weights and shear strength parameters are summarized below on **Table 6**.

Table 6
Protective Soil Cover and Compacted Low Permeable Soil Liner
Unit Weights and Strength Parameters

Layer	Moist Unit Weight γ_{moist}	Saturated Unit Weight γ_{sat}	Shear Strength Short-Term Conditions		Shear Strength Long-Term Conditions	
			Cohesion c	Friction Angle ϕ	Cohesion c'	Friction Angle ϕ'
Protective Soil Cover	129 pcf	132 pcf	720 psf	13.5°	720 psf	13.5°
Compacted Low Permeable Soil Liner	129 pcf	132 pcf	720 psf	13.5°	720 psf	13.5°

Consolidation Parameters for Compacted Low Permeable Soil Liner

It is assumed that the consolidation parameters of the compacted low permeable soil liner presented on **Table 7** below are equal to the consolidation parameters of the combined Stratum II-III-IV soil unit/layer as presented previously on **Table 2**.

Table 7
Compacted Low Permeable Soil Liner
Consolidation Parameters

Layer	Void Ratio (e_0)	Average Plasticity Index	Compression Index C_c	Recompression Index C_r	Secondary Compression Index C_α
Compacted Low Permeable Soil Liner	0.64	36	0.4204	0.0609	0.0136

Notes:

1. Void ratio of 0.64 represents an estimated approximate average based on laboratory test data (Reference No. 2).
2. Compression Index (C_c) was calculated using the following correlation (Reference No. 7): $C_c = 0.046 + (0.0104 \times PI)$
3. Recompression Index (C_r) was calculated using the following correlation (Reference No. 7): $C_r = 0.00194 \times (PI - 4.6)$
4. Secondary Compression Index (C_α) was calculated using the following correlation (Reference No. 7): $C_\alpha = 0.00168 + (0.00033 \times PI)$

Liner System Geosynthetics

The stability of the liner system geosynthetics will depend on interface shear strengths between the various geosynthetic components which will include from top-down: protective soil-to-geosynthetic, geosynthetic-to-geosynthetic, and geosynthetic-to-compacted soil liner. The liner system design proposes two different geosynthetic layer options for both the sideslope liner and base liner e. The critical geosynthetic interface will be between one of the following interfaces:

- Geosynthetics Interfaces on **3H:1V Sideslope Liner** (*from top-down*)
  - *Protective Soil Layer*
  - *Geosynthetics - Option 1*
    - Geotextile Slip Layer
    - Double-Sided Drainage Geocomposite
    - 60-mil Textured HDPE Geomembrane
  - *Geosynthetics - Option 2*
    - Geotextile Slip Layer
    - Double-Sided Drainage Geocomposite
    - Bentonite Enhanced Textured FML (bentonite side faced down)
    - Bentonite Enhanced Textured FML (bentonite side faced up)
  - *Compacted Low Permeable Soil Liner ($k \leq 1x10^{-7}$ cm/sec)*

- Geosynthetics Interfaces on **Base Liner** (*from top-down*)
  - *Protective Soil Layer*
  - *Geosynthetics - Option 1*
    - Double-Sided Drainage Geocomposite
    - 60-mil Textured HDPE Geomembrane
  - *Geosynthetics - Option 2*
    - Double-Sided Drainage Geocomposite
    - Bentonite Enhanced Textured FML (bentonite side faced down)
  - *Compacted Low Permeable Soil Liner ($k \leq 1x10^{-7}$ cm/sec)*

The critical interface shear strength was assumed equal to a friction angle of 8 degrees with zero cohesion for the liner sideslopes and equal to a friction angle of 14 degrees with zero cohesion for the liner base. The values were selected based on a review of past project laboratory test results for various interfaces of similar liner materials (**Reference No. 13**).

Table 8
Critical Geosynthetic Interface Shear Strength on Sideslope and Base Liner

Layer	Moist Unit Weight γ_{moist}	Saturated Unit Weight γ_{sat}	Shear Strength Short-Term Conditions		Shear Strength Long-Term Conditions	
			Cohesion c	Friction Angle ϕ	Cohesion c'	Friction Angle ϕ'
Critical Geosynthetic Interface Along Sideslope Liner	129 pcf	132 pcf	0 psf	8°	0 psf	8°
Critical Geosynthetic Interface Along Base Liner	129 pcf	132 pcf	0 psf	14°	0 psf	14°

Seismic Impact Zone

A seismic impact zone is defined as an area with a 10% or greater probability that the maximum horizontal acceleration in lithified earth material, expressed as a percentage of the earth's gravitational pull, will exceed 0.10g in 250 years. Maximum horizontal acceleration is defined as the maximum expected horizontal acceleration depicted on a seismic hazard map, with a 90% or greater probability that the acceleration will not be exceeded in 250 years.

From the United State Geologic Survey (USGS) Earthquake Hazards Program - National Seismic Hazard Mapping website, the seismic coefficient for the landfill site area was determined to be between 0.02g and 0.04g, expressed as a percentage of the earth's gravitational pull (**Reference No. 14**). Therefore the site is not in a seismic impact zone and seismic analyses are not required in accordance with Title 30 Texas Administrative Code (TAC) §330.557.

Safety Factors Assumed in Geotechnical Stability Calculations

A safety factor of 1.5 was assumed for critical loading conditions in all stability calculations (**Reference No. 15**). A safety factor of 1.0 was assumed to be adequate when using all worst case conditions. The foundation bearing capacity and sideslope liner runout calculations assumed a minimum safety factor of 2.0 for both the short-term and long-term shear strength conditions.

Water Surface Assumed in Geotechnical Stability Calculations

The existing water table surface was conservatively assumed to be at ground surface for the slope stability calculations and therefore was assumed as follows for the different slope stability scenarios:

- *Cell Development Scenarios* - the water surface is located at the bottom of the compacted low permeable soil liner layer along the liner sideslopes and liner base (*assumes dewatering to mass excavation / liner grades if water is encountered in landfill cell*); and
- *Complete Build-out / Final Landform Scenarios* - the combined water / leachate liquid level is located within the leachate drainage geocomposite or 1-inch above the compacted low permeable soil liner layer along the liner sideslopes and base.

The water table is believed to be perched and present only in isolated pockets across the site as determined from subsurface investigations performed on this site (**Reference No. 1**). The site boring logs indicate soils to be slightly moist to dry with only isolated pockets of wet to saturated soils present. Visual observations and photo logs (**Reference No. 1**) made of the test pits performed in 2012 show the soils to be extremely dry indicating a much lower water surface across the site.

Based on the results of site-specific investigations performed to date, the subsurface water is expected to pose little threat to successful excavation of the landfill cells. Further, little if any seepage is expected to occur based on observations made of isolated occurrences of pockets of wet to saturated soils on site that will produce very small volumes of water during cell excavation / development. Additionally, if seepage did occur it would most likely occur at a very slow rate of flow due to the very low permeability of the site soils (i.e., hydraulic conductivities ranging from 5.5 x 10^{-9}- to 8.3 x10^{-7} cm/ sec - **Reference No. 1**).

Summary of Material Unit Weights and Shear Strength

A summary of material unit weights and shear strength values for all landfill layers and geologic units directly beneath the landfill is presented on **Table 9** below.

Table 9
Summary of Material Unit Weights and Shear Strength

Layer Description	Total Unit Weight γ_{moist}	Saturated Unit Weight γ_{sat}	Shear Strength Short-Term Conditions		Shear Strength Long-Term Conditions	
			Cohesion c	Friction Angle φ	Cohesion c'	Friction Angle φ'
Soil Stratum I:						
Beneath Landfill Sideslope Liner, and outside of Landfill footprint	125 pcf	126 pcf	1,000 psf	0°	250 psf	10°
Soil Stratum II, III & IV:						
Beneath Landfill Sideslope Liners, Base Liners, and areas outside Landfill footprint	129 pcf	132 pcf	2,500 psf	5°	720 psf	13.5°
Landfill Layers:						
Final Cover	129 pcf	132 pcf	720 psf	13.5°	720 psf	13.5°
Waste (includes daily and intermediate cover)	65 pcf	65 pcf	0 psf	30°	0 psf	30°
Protective Soil Cover Layer (2-ft) on Sideslopes and Base	129 pcf	132 pcf	720 psf	13.5°	720 psf	13.5°
Compacted Low Permeable Soil Liner on Sideslopes and Base	129 pcf	132 pcf	720 psf	13.5°	720 psf	13.5°
Critical Geosynthetic Interface along Sideslope Liner	129 pcf	132 pcf	0 psf	8°	0 psf	8°
Critical Geosynthetic Interface along Base Liner	129 pcf	132 pcf	0 psf	14°	0 psf	14°

Summary of Material Consolidation Parameters

A summary of material consolidation parameters for all landfill layers and geologic units directly beneath the landfill is presented on **Table 10** below.

Table 10
Summary of Material Consolidation Parameters

Layer Description	Void Ratio (e_o)	Liquid Limit	Effective Overburden Pressure p'_o	Pre-Consolidation Pressure p'_c	Compression Index C_c (C'_c)	Recompression Index C_r	Secondary Compression Index C_α (C'_α)
Final Cover	0.64	58	--	--	0.4204	0.0609	0.0136
Compacted Low Permeable Soil Liner at 100-ft.bgs [1]	0.64	58	6,960 psf (333.25 kPa)	125,847 psf (6,026 kPa)	0.0609	0.0609	0.0136
Stratum II-III-IV at 150-ft.bgs [2]	0.64	58	10,440 psf (499.87 kPa)	114,763 psf (5,495 kPa)	0.4204	0.0609	0.0136
Waste Fill (includes daily and intermediate cover)	--	--	--	--	(0.25)	--	(0.051)

Notes

1. The referenced depth of 100-ft.bgs for the Compacted Low Permeable Soil Liner is relevant to the calculation of the effective overburden pressure and preconsolidation pressure.
2. The referenced depth of 150-ft.bgs for the Stratum II-III-IV soil is relevant to the calculation of the effective overburden pressure and preconsolidation pressure on the Stratum IV soil that lies 50-ft below the Compacted Soil Liner.

Reference Nos. 4, 5, and 6

Empirical Correlations Between
Plasticity Indices & Shear Strength Values

Technically Complete, March 11, 2016

AN INTRODUCTION TO

Geotechnical Engineering

Robert D. Holtz
William D. Kovacs

Prentice-Hall Civil Engineering and Engineering Mechanics Series

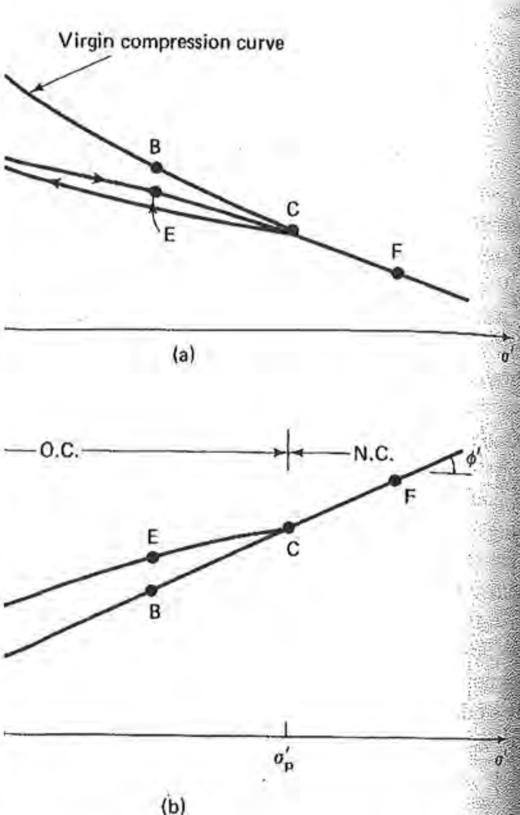

ssion curve; (b) Mohr failure envelope (DEC) for
ay.

call from Fig. 8.4 that the virgin compression
etically is concave upward.) Let us assume that
a sedimentary clay at a very high water content
continue to increase the vertical stress we reach
ıpression curve and conduct a CD triaxial test.
he same thing with a CD direct shear test.) The
ısolidated to point A on the virgin curve would
he normally consolidated Mohr failure envelope.
ısolidate and test another otherwise identical

specimen which is loaded to point B, then we would obtain the strength, again normally consolidated, at point B on the failure envelope in Fig. 11.26b. If we repeat the process to point C (σ_p', the preconsolidation stress), then rebound the specimen to point D, then reload it to point E and shear, we would obtain the strength shown at point E in the lower figure. Note that the shear strength of specimen E is greater than specimen B, even though they are tested at exactly the same effective consolidation stresses. The reason for the greater strength of E than B is suggested by the fact that E is at a lower water content, has a lower void ratio, and thus is denser than B, as shown in Fig. 11.26a. If another specimen were loaded to C, rebounded to D, reloaded back past E and C and on to F, it would have the strength as shown in the figure at point F. Note that it is now back on the virgin compression curve and the normally consolidated failure envelope. The effects of the rebounding and reconsolidation have been in effect *erased* by the increased loading to point F. Once the soil has been loaded well past the preconsolidation pressure σ_p', it no longer "remembers" its stress history.

11.9.2 Typical Values of Drained Strength Parameters

For the Mohr failure envelopes of Figs. 11.25 and 11.26 we did not indicate any numerical values for the effective stress strength parameters ϕ'. Average values of ϕ' for undisturbed clays range from around 20° for normally consolidated highly plastic clays up to 30° or more for silty and sandy clays. The value of ϕ' for compacted clays is typically 25° or 30° and occasionally as high as 35°. As mentioned earlier, the value of c' for normally consolidated non-cemented clays is very small and can be neglected for practical work. If the soil is overconsolidated, then ϕ' would be less, and the c' intercept greater than for the normally consolidated part of the failure envelope (see Fig. 11.26b again). According to Ladd (1971b), for natural overconsolidated non-cemented clays with a preconsolidation stress of less than 500 to 1000 kPa, c' will probably be less than 5 to 10 kPa at low stresses. For compacted clays at low stresses, c' will be much greater due to the prestress caused by compaction. For stability analyses, the Mohr-Coulomb effective stress parameters ϕ' and c' are determined over the range of effective normal stresses likely to be encountered in the field.

It has been observed (for example, Kenney, 1959) that there is not much difference between ϕ' determined on undisturbed or remolded samples at the same water content. Apparently, the development of the maximum value of ϕ' requires so much strain that the soil structure is broken down and almost remolded in the region of the failure plane.

Empirical correlations between ϕ' and the plasticity index for normally consolidated clays are shown in Fig. 11.27. This correlation is based

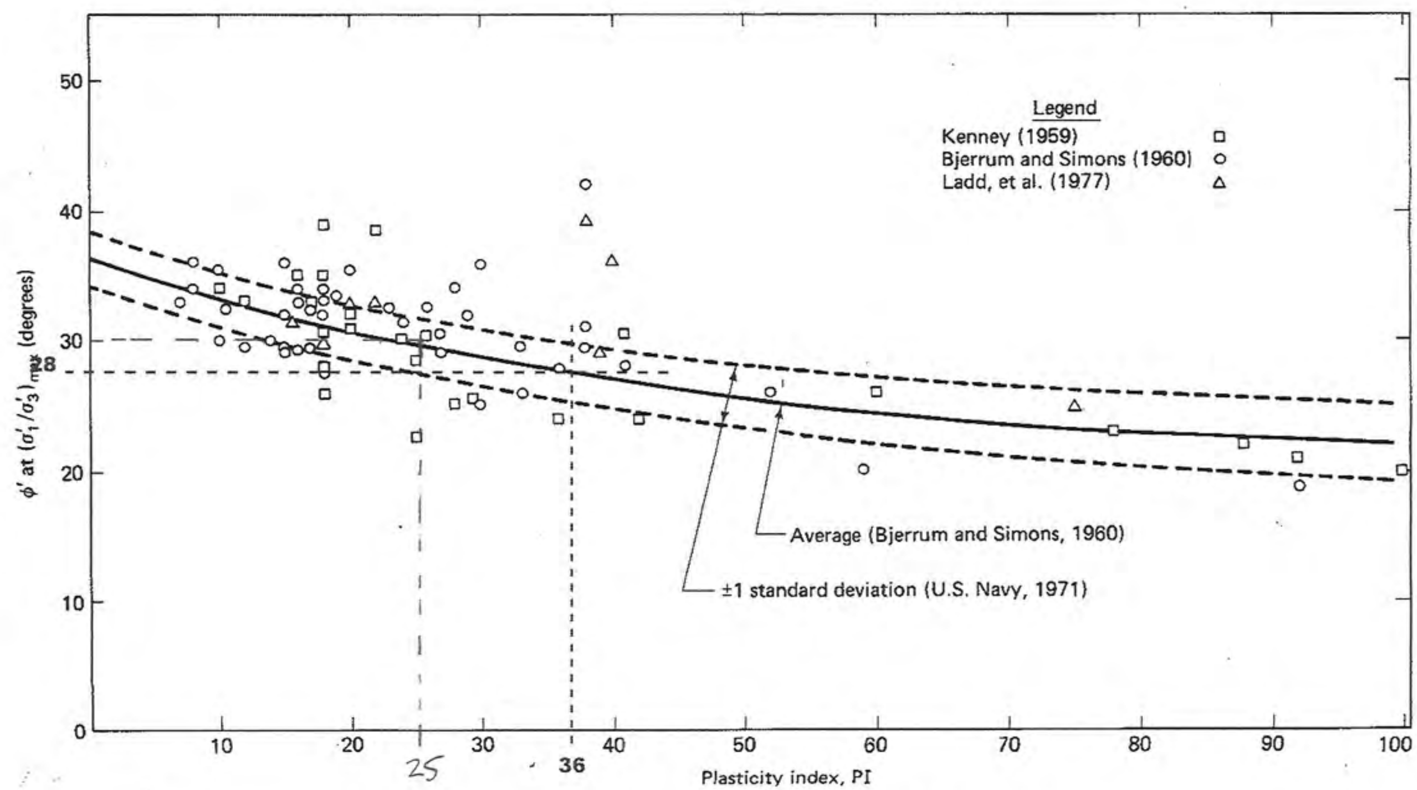

Fig. 11.27 Empirical correlation between φ' and PI from triaxial compression tests on normally consolidated undisturbed clays (after U.S. Navy, 1971, and Ladd, et al., 1977).

SOIL MECHANICS IN ENGINEERING PRACTICE

THIRD EDITION

Karl Terzaghi
Ralph B. Peck
Gholamreza Mesri

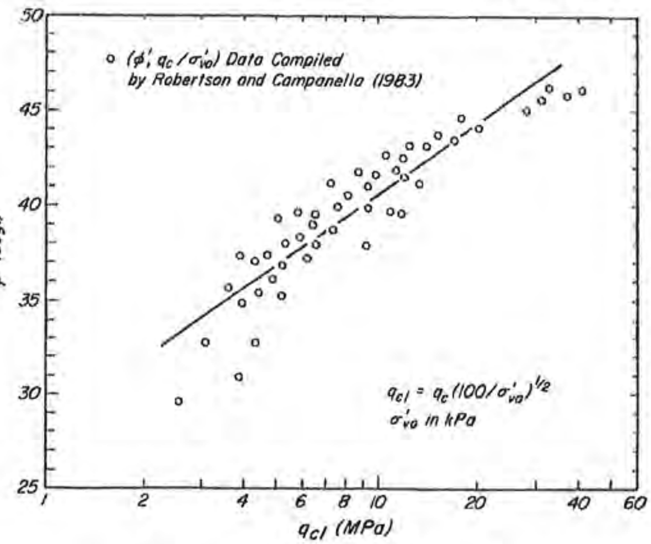

Figure 19.5 Empirical correlation between friction angle ϕ' of sands and normalized push cone tip penetration resistance.

ory (de Beer 1948, Meyerhof 1961, Janbu and Senneset 1974, Durgunoglu and Mitchell 1975, Mitchell and Keaveny 1986). Data compiled by Robertson and Campanella (1983) are plotted in terms of q_{c1} in Fig. 19.5. The correlation is mainly applicable to normally consolidated young sand deposits composed of quartz and feldspars. It underestimates by several degrees the friction angle of compressible carbonate sands with crushable particles, and it overestimates by several degrees the friction angle of overconsolidated or aged sands with values of σ'_{ho} higher than those in normally consolidated young deposits (Schmertmann 1975).

The correlation between ϕ' and $(N_1)_{60}$ in Fig. 19.6 is based on various proposals for the relationship between ϕ' and standard penetration blow count N (Peck et al. 1953, De Mello 1971, Schmertmann 1975, Stroud 1988). It underestimates ϕ' for calcareous sands with crushable particles and overestimates ϕ' for overconsolidated sands (Stroud 1988). Figure 19.6 also includes relations between ϕ' and $(N_1)_{60}$ determined from the empirical correlation in Fig. 19.6 together with q_c/N_{60} values of 400 and 500 kPa for sand deposits. The two different empirical correlations between ϕ' and q_c and between ϕ' and N_{60}, which have originated from separate databases, lead to comparable values of ϕ' for sands.

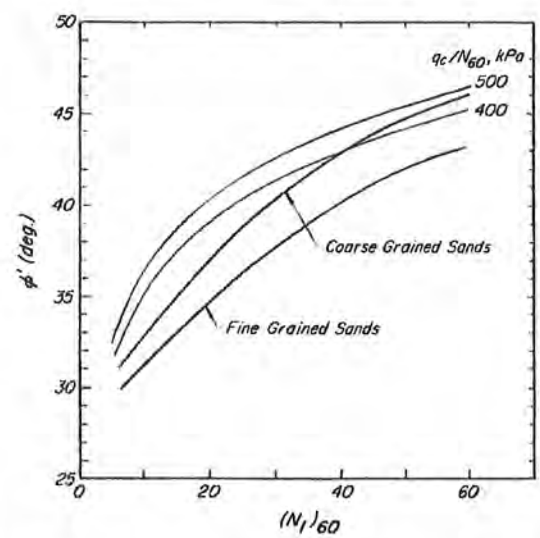

Figure 19.6 Empirical correlation between friction angle ϕ' of sands and normalized standard penetration blowcount.

19.2 Drained Shear Strength of Cohesive Soils

The drained shear strength of normally consolidated cohesive soils is defined by the friction angle ϕ', as follows:

$$s = \sigma' \tan \phi' \qquad (19.6)$$

The effective normal stress σ' on the plane of shear is determined by the total normal stress and the equilibrium hydrostatic or steady porewater pressure condition. The friction angle ϕ', which corresponds to a more or less random arrangement of particles, is mainly a function of the clay mineral content and clay mineralogy of the composition. Values of ϕ' for the full range of clay compositions are shown in Fig. 19.7. Among the pure clay minerals, sodium montmorillonite (consisting of filmy particles) has the lowest value of ϕ', whereas attapulgite (with interlocking fibers) exhibits the highest value. Typical values of ϕ' for soft clay, stiff clay, and shale constituents are in the range of 25° to 35°, 20° to 35°, and 15° to 35°, respectively. The water-filled and rough surface-

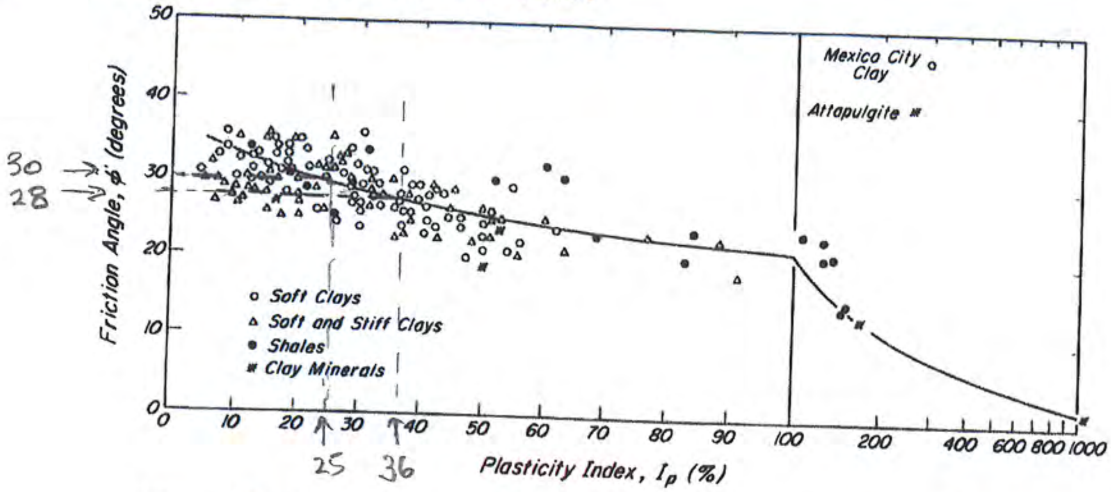

Figure 19.7 Values of friction angle ϕ' for clays of various compositions as reflected in plasticity index.

textured diatom shell fragments that make up the matrix of Mexico City clay are capable of generating unusually large friction angles while retaining an exceptionally large amount of water. At each plasticity index, different values of ϕ' result from the difference in clay size fraction of soils and from the difference in effective normal stress at which ϕ' was measured. The high values of ϕ' correspond to soils with clay size fraction of less than 20% and effective normal stresses less than 50 kPa. The low values are representative of soils with clay size fraction of greater than 50%, subjected to effective normal stresses of higher than 400 kPa. Torsional ring-shear tests by Stark and Eid (1994) show that ϕ' may decrease by 4° as the clay size fraction increases from less than 20% to more than 50% or as effective normal stress increases from less than 50 kPa to more than 400 kPa. Although there is a strong correlation between friction angle and plasticity index, the significant scatter of the data around the empirical relationship shown in Fig. 19.7 indicates that ϕ' should be measured directly on major projects. The drained triaxial compression test on specimens normally consolidated under an equal all-around pressure is most suitable for determining ϕ'.

The drained shear strength of an overconsolidated clay should ordinarily be greater than the drained strength of the same constituents in a normally consolidated state, mainly because the overconsolidated clay has a smaller preshear void ratio. However, the mobilized or available drained shear strength of heavily overconsolidated clays strongly depends on their condition before shear and when they reach failure. An overconsolidated clay mobilizes its intact strength at failure only if it has remained in an intact condition during geological unloading and associated swelling, remains intact in response to a construction operation that eventually leads to a failure, and reaches its peak resistance at the instant of a global instability.

On the other hand, an overconsolidated clay has available at the instant of slip only its fully softened shear strength if it has been badly fissured and jointed during the removal of overburden or of lateral support by erosion, has softened further in response to an excavation process that leads to a long-term drained failure, or has been involved in severe progressive failure. An overconsolidated clay mass that has already experienced large displacements along a major plane of shear can mobilize only the residual shear strength if movements are reactivated along the preexisting shear surface. The presence in the fabric of an overconsolidated cohesive soil of discontinuities, such as brecciations, slickensides, fissures, joints, and shears, becomes an increasingly important factor in relation to the available drained shear strength at failure as preconsolidation pressure, overconsolidation ratio, plasticity, and, therefore, stiffness and brittleness increase.

19.2.1 Intact Shear Strength

The drained intact shear strength of a saturated overconsolidated clay is commonly expressed in terms of the intercept c' and the angle ϕ' of a failure envelope in the Mohr diagram, as

$$s = c' + \sigma' \tan \phi' \qquad (19.7)$$

In general the angle ϕ' in Eq. 19.7 is not comparable to the friction angle in Eq. 19.6. An example of a failure envelope for an intact sample of an overconsolidated London clay is shown in Fig. 19.8. The sample was taken from a depth of 35 m below ground level, and the best estimates of σ'_{vo} and σ'_p are 390 kPa and 4100 kPa, respectively. London clay was deposited under marine conditions in the Eocene period about 30 million years ago. Subsequently, uplift and erosion in Tertiary and Pleistocene times removed 170 m to 340 m of overlying sediments. The failure envelope of the overconsolidated clay

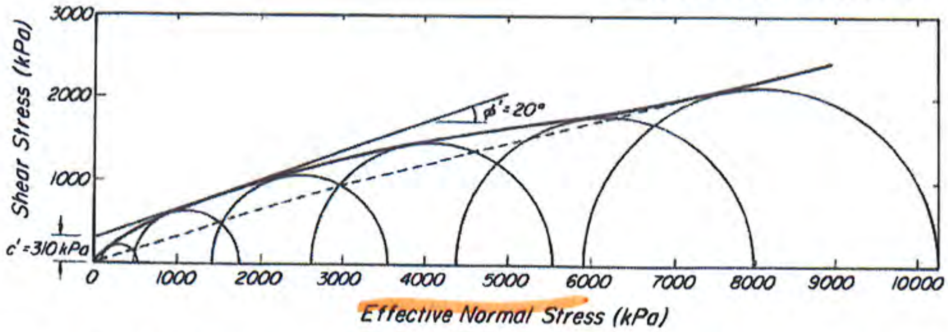

Figure 19.8 Mohr envelope for a sample of intact London clay from a depth of 35 m (data from Bishop et al. 1965).

shows a very marked curvature before it merges with the envelope corresponding to the normally consolidated condition. There is a significant change in slope and intercept in passing from a low-stress to a high-stress range: c' and ϕ' change from 100 kPa and 30°, respectively, in the lower range to 790 kPa and 10° in the upper range. This type of nonlinear failure envelope is characteristic of the intact shear strength of overconsolidated soft clays, stiff clays, and shales. Therefore, in reporting the values of c' and ϕ', the effective normal stress range to which they correspond must be specified. For example, in Fig. 19.8 the combination $c' = 310$ kPa, $\phi' = 20°$ corresponds only to the σ' range of 1000 to 2000 kPa. Outside this range, the same set of strength parameters would greatly overestimate the intact strength of this clay.

Because the intact strength envelope depends strongly on the preconsolidation pressure and overconsolidation ratio, a summary of such strengths for a variety of overconsolidated soft and stiff clays and shales in terms of the values of c' and ϕ' has little meaning. For this reason, the drained strength of an overconsolidated clay is expressed in terms of the drained strength of the same constituents in the normally consolidated state as

$$s = \sigma' \tan \phi' \cdot \mathrm{OCR}^{1-m} \qquad (19.8)$$

According to Eq. 19.8, the drained intact strength of an overconsolidated clay is greater by a factor of OCR^{1-m} than the drained shear strength of the same constituents in a normally consolidated state as given in Eq. 19.6. The overconsolidation ratio, OCR, in Eq. 19.8 is defined in terms of the effective normal stress at which the failure envelope of the overconsolidated clay joins the envelope for the normally consolidated condition.

Values of the exponent m for soft and stiff clays and shales are presented in Table 19.4. The term intact refers to completely undisturbed and unfissured materials, whereas *destructured* describes slightly fissured stiff clays and shales, and soft clays that have been sheared beyond the yield surface to a large-strain condition. Destructured does not refer to fully softened stiff clays and shales or

Table 19.4 Values of m in Eq. 19.8

Material	m Intact	m Destructured
Cemented soft clays	0.4–0.5	0.5–0.7
Stiff clays and shales	0.5–0.6	0.6–0.8
Soft clays	0.6–0.7	0.7–0.9

remolded soft clays for which the values of m are expected to range from 0.9 to 1. The lowest values of m are obtained for bonded or cemented soft clays such as those of eastern Canada. Beneath level ground such clays exhibit OCR values between 1.5 and 3, whereas in natural or cut slopes the OCR ranges from 2 to 20. The low values of m define the portion of the failure envelope above the normally consolidated strength envelope (Eq. 19.6).

Frequently the available intact strength is significantly modified by fissuration and softening. The considerable variation in strength of what is believed to be intact material is most likely associated with the degree of fissuring of the clay. This is best illustrated by a comparison of drained strengths of undisturbed samples of an overconsolidated clay taken from various depths below the ground surface. For London clay, peak strength parameters in the effective normal stress range of 100 kPa to 600 kPa, as measured in 60-mm direct shear tests or 38-mm-diameter triaxial compression tests, are compared in Table 19.5. A change in the nature and scale of the fissure pattern accounts for the marked decrease in the value of c' as the depth decreases. For London clay the mean spacing of the randomly oriented fissures decreases and the number of fissures per unit volume increases as the upper surface of the clay is approached. This suggests that stress release together with chemical and physical weathering play an important role in the genesis of fissures. Fissures within the top 12 m of London clay are typically between 25 and 75 mm long and rarely exceed

Table 19.5 Intact Strength of London Clay, as Modified by Fissuration

	Values of Parameters in Eq. 19.7	
Depth (m)	c' (kPa)	ϕ'
2–3	7	20°
3–7	15	20°
7–10	31	20°
35	100	30°

150 mm; at the lower elevations, the fissures are more widely spaced. Beneath level ground high lateral pressures tend to keep the fissures closed, whereas in areas of sloping ground lateral stress release may lead to their opening.

Large slopes of failure envelopes for intact samples in the low effective stress range, such as 30° for London clay in Table 19.5, reflect the aggregated nature of the fabric of intact overconsolidated clay and interparticle friction resulting from interlocking of the aggregations. These slopes may give a misleading impression of the frictional characteristics of the components of the clay, which are reflected in a more meaningful way by the normally consolidated or fully softened ϕ' in Eq. 19.6, or the residual friction angle ϕ'_r. Data in Table 19.5 also show that before large displacements concentrate along a major plane of shear, the slope of the intact failure envelope does not drop below the fully softened friction angle, the value of which for London clay is near 20°. Thus, for fissured clays, the difference in degree of fissuration is mainly reflected in the magnitude of the cohesion intercept c'.

The intact strength of nonfissured overconsolidated clays is independent of the size of undisturbed specimens used to measure it. It is also independent of whether drained tests or undrained tests with porewater pressure measurements are carried out. On the other hand, where the spacing of the fissures is small in comparison with the size of the specimens, the drained shear strength of a fissured clay, such as that encountered at shallow depths in London, strongly depends on the size of the specimen in relation to the fissure spacing. The influence of the ratio of specimen size to fissure spacing is reflected mainly in the measured value of c'; small specimens with low frequency of fissures generally indicate large values of c'. This creates a serious problem in measuring and selecting strength parameters for stability analyses in overconsolidated clays. Gradual opening or elongation of fissures resulting from the effects of excavation or sampling disturbance, including delay in testing, can lead to an underestimation of the intact strength available *in situ*. For example, on the assumption that London clay at a depth of 35 m below ground surface is practically free from fissures, the intact strength measured using high-quality block samples, as shown in Fig. 19.6, should be available at that depth to provide the bearing capacity of deep bored cylindrical foundations that are constructed in place without disturbing the clay or allowing time for the fissures to open. One mechanism, however, that could lead to an available strength at 35-m depth less than the intact strength in Fig. 19.8 is progressive failure along a global slip surface, because the overlying fissured zones may require higher strain to mobilize their peak strength.

More often, fissures lead to an overestimation of the available strength in full-scale field problems, because laboratory tests can rarely be made on samples large enough to be representative of the fissured nature of the clay. This is especially important for excavations and cut slopes less than 10 to 20 m deep. Both drained long-term and short-term strengths of a fissured clay mass can be appreciably lower than the strength of the intact clay between the fissures. There is abundant evidence that in overconsolidated fissured clays the cohesion intercept c' prevailing at the time of a long-term drained failure is far less than the value measured in conventional laboratory tests on small specimens (Mesri and Abdel-Ghaffar 1993). For London clay the ratio of the short-term strength of fissured and jointed clay masses in the field to the undrained strength measured on 38-mm-diameter triaxial compression specimens is in the range of 55% to 75%. Back analyses of first-time slope failures in London clay suggest that even the drained strength measured on large-diameter samples overestimates the strength available on the slip surface in the field. A value of c' equal to 7 kPa was measured using triaxial compression specimens up to 260 mm in diameter, as compared with the back-calculated c' of only 1.0 kPa from the average field strength mobilized when a slope failure occurred. The angle ϕ' was assumed to be 20° in both cases. In excavated slopes it is possible that, during the decades that are required for the increase in porewater pressure from the initially low values following stress reduction during excavation to the steady seepage values, fissures open as a result of small movements associated with the removal of lateral support. The clay may soften along these fissures until global failure occurs. Another factor that can contribute to a lower c' available on a slip surface is progressive failure induced by the joints and fissures.

The decrease in cohesion intercept c' by fissuration or other weathering mechanisms in overconsolidated clay is related to the difference between fully softened ϕ' and residual ϕ'_r. For London clay, which has a ϕ'_r value of about one-half ϕ', fissuration has a significant effect on the drained strength, reflected in a small value of c'. On the other hand, in low plasticity boulder clays of glacial origin ($I_p < 20\%$) as well as silty soft clays in eastern

Canada, the postpeak large-strain values of c' in the range of 5 to 10 kPa measured in laboratory tests are also mobilized in long-term slope failures in the field. Most of the clay fraction in these clays is composed of mechanically pulverized rock flour. For clays of low plasticity, Fig. 19.7 shows that the values of ϕ' are near 30°, and according to Fig. 19.16 the difference between ϕ_r' and ϕ' is small. This suggests that clays with low clay content and plasticity are generally unfissured or, as discussed later, that the small difference between ϕ' and ϕ_r' minimizes the influence of fissures on available shear strength. Typical unsheared fissures and joints exhibit a matt surface texture. In London clay this consists of mounds and depressions of the order of 0.1 mm high and 0.2 to 0.4 mm in diameter, without clay-particle reorientation at the fissure surface. However, some fissures are slickensided with a polished and striated surface, or are coated with a thin clay gouge. These features suggest some particle orientation on particular fissures during the mobilization of peak strength.

In summary, whenever the intact strength is used in design or analysis, the significance of existing or potential fissures on the c' available during a global instability must be examined. The size of the specimen in tests for the measurement of drained strength should reflect, as much as is practically feasible, the frequency of fissures in the field. Further reductions in the measured c' may be necessary to take into account the possible influence of progressive failure, because c' and ϕ' of even a representative specimen may not be mobilized simultaneously on all segments of a global slip surface. Whenever reliance is placed on c' for stability of a mass of clay, local experience should be examined carefully or a conservative approach adopted.

In unsaturated soils that are not submerged or flooded, a suction is imposed on the soil by the moisture-deficient environment which denies the soil full access to water. In unsaturated soils with air voids connected to the atmosphere, the total normal stress acts as an effective confining pressure and pushes the soil particles together. In such a soil, and at a constant suction, the increase in shear strength with increasing total normal stress is determined by the friction angle ϕ'. This is illustrated in Fig. 19.9 by a series of suction-controlled direct shear tests on Guadalix Red clay (Escario et al. 1989). At zero suction, the saturated undisturbed clay displays a cohesion intercept c'. On the other hand, Fig. 19.10 shows that at a constant normal stress, the increase of shear strength with increasing suction becomes insignificant even in the practical range of suction values up to 4 MPa. The initial slope of the s vs u_s relationship is equal to $\tan \phi'$, because at $u_s = 0$ the soil is saturated, and an increment of suction represents a decrease in porewater pressure or an increase in effective stress. However, as the suction increases and the soil becomes unsaturated, the Terzaghi relation (Eq. 15.2) between effective stress and porewater pressure

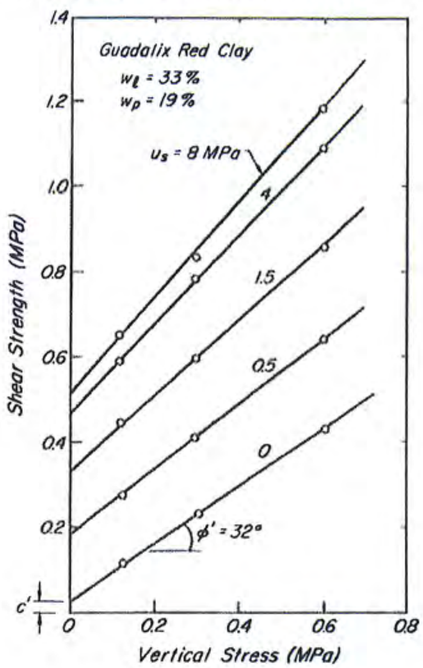

Figure 19.9 Results of direct shear tests with suction control on Guadalix red clay (data from Escario et al. 1989).

becomes invalid, and a decrease occurs in the component of suction that pulls the soil particles together and generates shearing resistance. For practical purposes, the drained shear strength of unsaturated soils may be expressed as (Abramento and Carvalho 1989)

$$s = c' + \sigma \tan \phi' + b\, u_s^a \tag{19.9}$$

Laboratory shear-strength measurements on undisturbed and compacted unsaturated soils in the range of suction up to 4 MPa lead to a mean value of $a = 0.5$ and values of b in the range of 2 to 10 (Fig. 19.11). Equation 19.9 and Fig. 19.9 suggest that, at a constant suction, the suction-related shear-strength term is equivalent to a cohesion intercept that is permanently available only in the absence of submergence or a flooding. For example, for a soil with $\phi' = 30°$, a value of $b = 6$ (Fig. 19.11), together with $a = 0.5$ and a modest suction of 100 kPa, indicate a significant suction-related cohesion intercept of 60 kPa. This explains why slopes in unsaturated residual soils may be steep, and why shallow failures occur in these slopes in the rainy seasons as the soil becomes saturated and suction is lost.

19.2.2 Fully Softened Shear Strength

The fully softened drained shear strength of an overconsolidated clay, which may develop under highly fissured and jointed conditions without the presence of a preexisting shear surface, is defined by Eq. 19.6. It is equal to the friction angle ϕ' of clay of the same composition in a normally consolidated state, such as that produced by

 Technically Complete, March 11, 2016

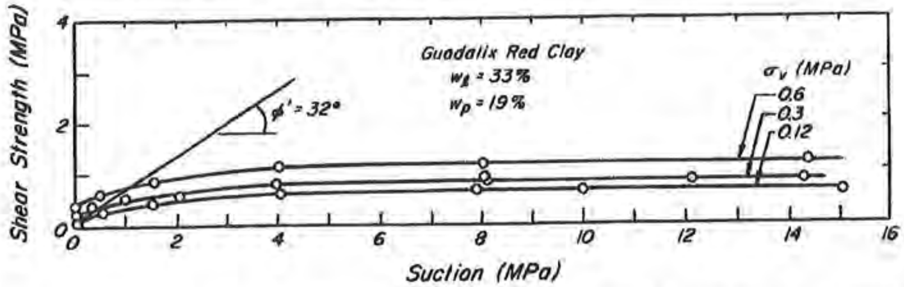

Figure 19.10 Influence of suction on shear strength at constant vertical-pressure Guadalix red clay (data from Escario et al. 1989).

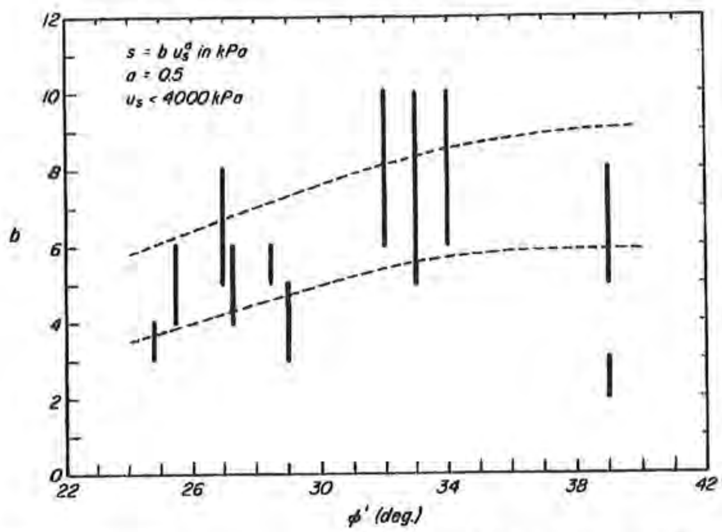

Figure 19.11 Summary of shear-strength measurements with suction control on undisturbed and on compacted unsaturated soils.

laboratory consolidation from a slurry. The failure envelope of a normally consolidated clay or the fully softened strength envelope, like those in Figs. 19.8 and 19.12, exhibits a slight curvature that indicates a decrease in ϕ' with increasing effective normal stress. Even in the random fabric that corresponds to the fully softened condition, increased effective confining pressure leads to increased face-to-face and reduced edge-to-face interaction among the plate-shaped particles. This results in decreased frictional resistance. For the normally consolidated London clay composition represented in Fig. 19.8, ϕ' starts at 21° in the low-pressure range, whereas it has a value of 17° at high effective normal stresses. Back analyses of first-time slides in stiff fissured clays on the basis of a value of fully softened ϕ' from laboratory tests at moderately high effective normal pressures and the best estimate of steady porewater pressure conditions may indicate a small cohesion intercept c'. For example, back analyses of first time slides in London clay, using $\phi' = 20°$ and values of pore pressure taken as $0.3\sigma_{vo}$, suggest a value of $c' = 1$ kPa (Fig. 19.13). Such a result indicates that the fully softened failure envelope was slightly nonlinear, or that a drained strength slightly greater than the fully softened value was available at the time of the slips. That is, either the assumed ϕ' slightly underestimated the fully softened ϕ' within the effective normal pressure range of less than 50 kPa, or a small cohesion intercept had survived fissuration and progressive failure.

The fully softened failure envelope for an overconsolidated clay can be determined by using intact specimens, intact specimens containing a distinct fissure or joint, or reconstituted normally consolidated specimens (Fig. 19.14). For samples consolidated from a slurry and for shear tests along a fissure or joint, the peak strength defines the fully softened failure envelope. When intact specimens are used, or when specimens are remolded at water contents less than the liquid limit, the fully softened strength corresponds to the postpeak shear stress at which the increase in water content during shear levels off. Both drained tests and undrained tests with porewater pressure measurements can be used to define the fully softened failure envelope. The triaxial compression test is suitable for practically every type

Technically Complete, March 11, 2016

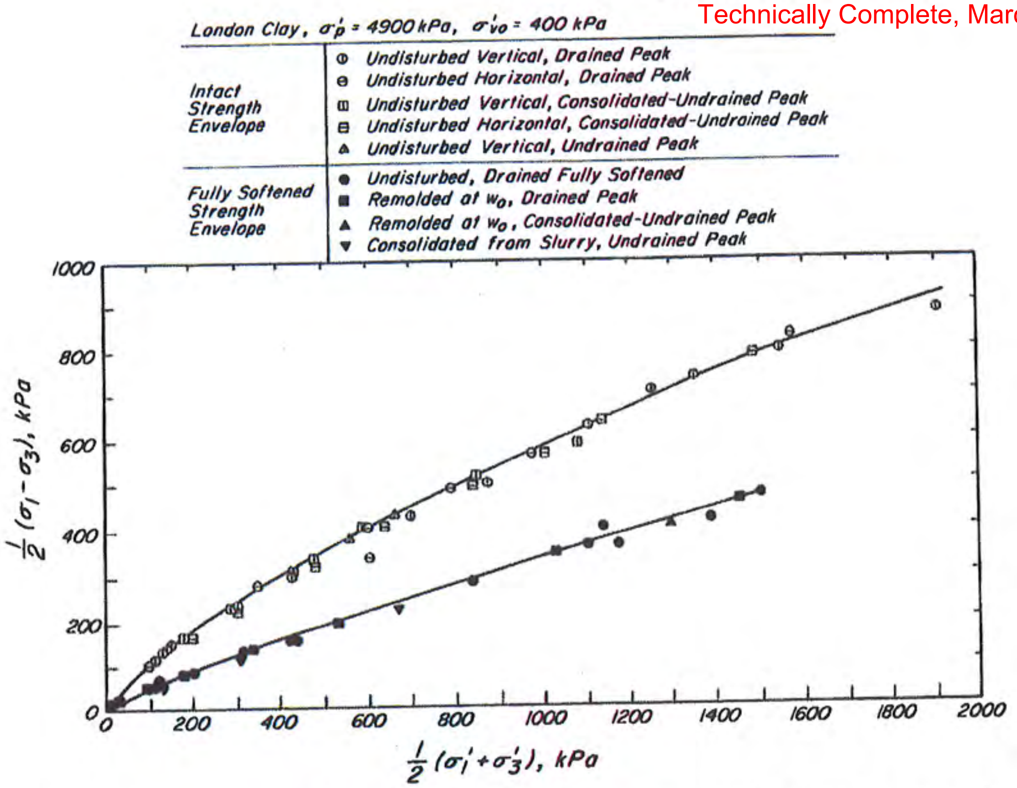

Figure 19.12 Intact and fully softened strengths of samples of London clay from depth of 35 m (Bishop et al. 1965).

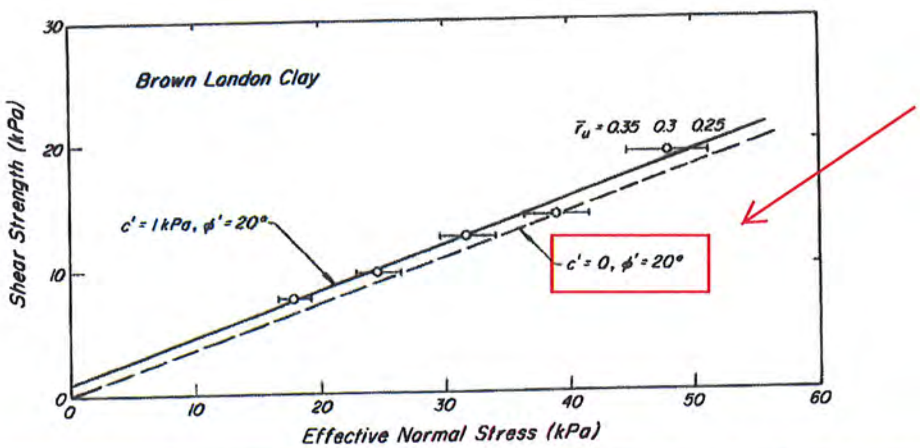

Figure 19.13 Fully softened shear strengths of brown London clay back-calculated from first-time slides in cuts more than 45 years old (after Skempton 1977).

of specimen and for drained as well as undrained tests. The direct shear test (Article 17.3.2) may be useful for specimens containing a single distinct fissure or joint. However, specimens remolded at a water content higher than the liquid limit or specimens normally consolidated from slurry are preferred for the measurement of fully softened shear strength. Special care must be exercised on intact specimens to achieve, in the shear zone at the fully softened condition, complete porewater pressure equilibration and softening in drained tests, or complete porewater pressure equalization in undrained tests. Moreover, for intact samples, it may be difficult to define the area of the shear zone and to control axial loads after the formation of distinct shear planes.

Technically Complete, March 11, 2016

J. Michael Duncan
Stephen G. Wright
Thomas L. Brandon

SOIL STRENGTH and SLOPE STABILITY

SECOND EDITION

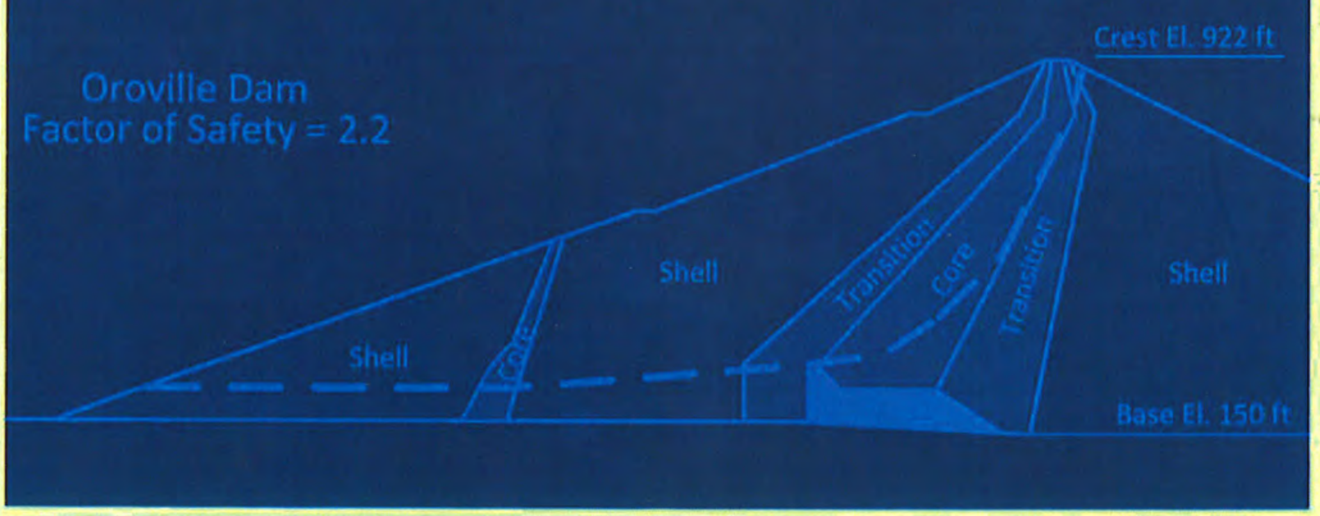

WILEY

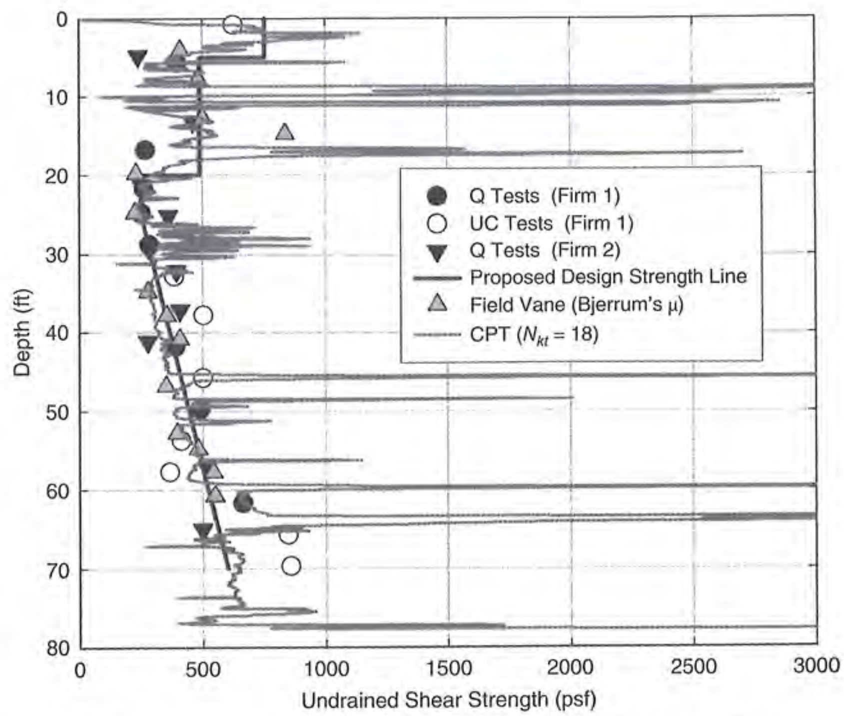

Figure 5.40 Undrained shear strength determined by Q, UCT, VST, and CPT for a New Orleans site.

The results of various methods of undrained strength determination for a site in New Orleans are shown in Figure 5.40. For this site, Q tests, UCTs, and field vane shear tests, were in good agreement. The CPT test results were calibrated using the vane shear test results and agree closely with them as a result. It can be seen that the CPT results show some large excursions from the general trend of strength with depth. This occurs because the clay is overlain by a marsh deposit that includes fibrous material, and, at depth, the deposit contains thin layers or lenses of granular material—nonplastic silt or fine sand—which increase the cone penetration resistance locally. It is unlikely that these thin layers would have any effect on slope stability, and they are usually ignored.

5.4.4 Use of Correlations for Estimating Undrained Shear Strength

Many correlations are available to estimate the undrained shear strength or undrained strength ratio of saturated clays. One of the earliest was proposed by Skempton (1957), relating the undrained strength ratio of normally consolidated clays to the Plasticity Index. This correlation, which was developed primarily using field vane shear tests and unconfined compression tests, is shown in Figure 5.41. The figure precedes development of Bjerrum's vane shear correction and for that reason probably overestimates the values of the undrained strength ratio for large values of Plasticity Index.

Because the undrained strength of saturated clays increases with increasing preconsolidation stress, characterizing the strengths of these materials in a way that includes the effect of preconsolidation pressure is very useful. Mesri (1989) found an approximately linear relationship between the strength and preconsolidation pressure for clays, which he expressed as

$$s_u = 0.22\sigma'_p \qquad (5.22)$$

with σ'_p is the preconsolidation pressure or maximum past effective stress. The constant 0.22 is a generalized undrained strength ratio for clay soils in an overconsolidated condition. Since the OCR is equal to the ratio of preconsolidation pressure to vertical effective stress, Mesri's equation can be also be written as

$$\frac{s_u}{\sigma'_v} = 0.22\,(\mathrm{OCR}) \qquad (5.23)$$

Jamiliokowski et al. (1985) presented an equation in a similar format, but with the OCR raised to an exponent of 0.8 and the undrained strength ratio for the soil in a normally consolidated condition estimated to be 0.23. This equation, shown below, seems to provide greater accuracy for higher values of OCR than Mesri's equation. This equation is often called the SHANSEP equation:

$$\frac{s_u}{\sigma'_v} = 0.23\,(\mathrm{OCR})^{0.8} \qquad (5.24)$$

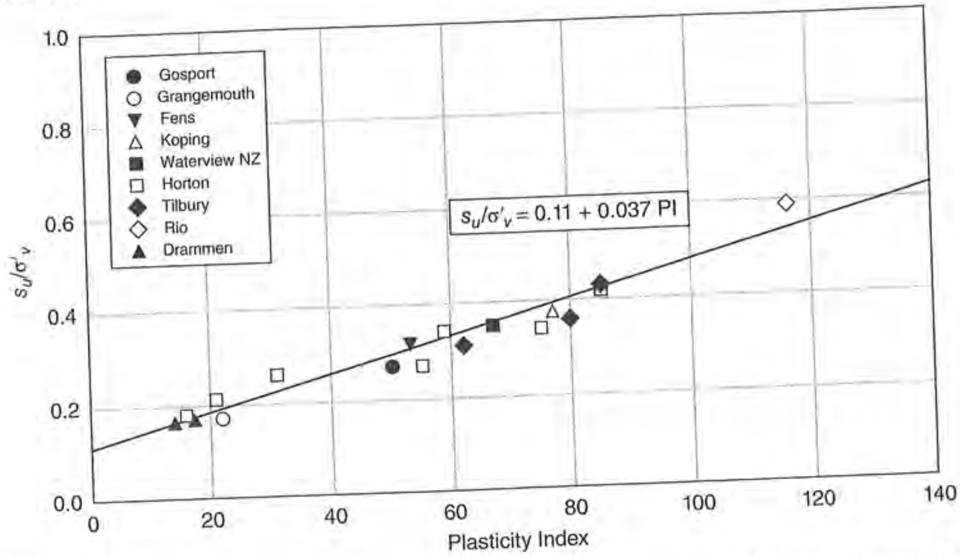

Figure 5.41 Skempton's (1957) correlation of undrained strength ratio with Plasticity Index (after Skempton, 1957).

This equation can be written in the generalized form:

$$\frac{s_u}{\sigma'_v} = S(\text{OCR})^m \tag{5.25}$$

where S is the undrained strength ratio for the soil in the normally consolidated condition, and m is an empirical exponent. Both S and m can be varied to fit laboratory test data for a particular site.

Use of SHANSEP for Undrained Strength Determination In some respects, the SHANSEP procedure can be viewed as a method to develop a site-specific correlation relating undrained strength to the overconsolidation ratio. It addresses the effects of disturbance, stress-induced anisotropy, and strain rate.

In order for the SHANSEP procedure to provide meaningful results, a number of conditions are necessary. First, it is necessary to know in detail the preconsolidation stress profile of the clay layer. Second, the SHANSEP procedure depends on the assumption that the soil will exhibit *normalized behavior*. This means that, for the case of a normally consolidated soil, the undrained strength ratio (s_u/σ'_v) should be the same if the sample is consolidated to $1.5\sigma'_v$ or $2.0\sigma'_v$, assuming that the test specimen is on the virgin compression curve at σ'_v in the ground, and at $1.5\sigma'_v$ and $2.0\sigma'_v$ in the laboratory.

Clays that are sensitive or highly structured do not normalize. Ladd and DeGroot (2003) state that the SHANSEP method will underestimate the undrained strength ratio for structured normally consolidated clays by 15 to 25 percent. It should also be noted that the SHANSEP procedure is intended to be applied to "fairly regular deposits for which a well-defined stress history can be obtained." Ladd and Foott (1974) state that "if a random deposit is encountered, the method is useless."

Sample Disturbance The SHANSEP method addresses sample disturbance by reconsolidating the laboratory test specimen to higher stresses than in situ but to the same value of the OCR. The SHANSEP method was not intended to determine the shear strength at a point, per se, as does an unconfined compression test. Rather, it is intended to determine the variation of the undrained strength ratio of the clay with the OCR, which can be applied to the entire clay deposit based on the stress history profile. An idealized plot of the consolidation process used in the SHANSEP procedure is shown in Figure 5.42*a* for a normally consolidated soil and Figure 5.42*b* for an overconsolidated soil.

If the SHANSEP procedure is to be used, it is important that the soil "normalizes." In the original SHANSEP paper by Ladd and Foott (1974), the decision as to whether or not a clay normalizes, and therefore is or is not suitable for the SHANSEP procedure, was to be evaluated through a qualitative assessment by the engineer. The procedure described by Coatsworth (1985) is preferable. Coatsworth (1985) suggested that a convenient method of examining if a soil normalizes, as well as of gauging the degree of disturbance, is to plot the undrained strength ratio versus the ratio of the laboratory consolidation stress to the preconsolidation pressure. Ratios of consolidation stress to preconsolidation pressure of 1.5, 2.5, and 4.0 can be used. Figure 5.43 shows hypothetical example plots for different combinations of disturbance and normalization that can be expected.

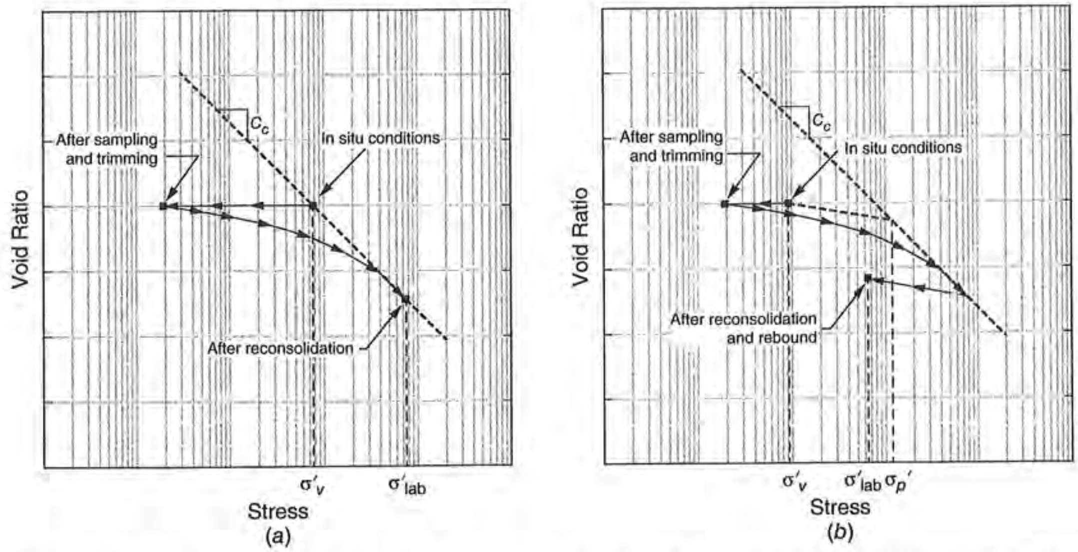

Figure 5.42 Idealized plot showing the path taken by (*a*) normally consolidated and (*b*) overconsolidated laboratory test specimens from field conditions to the end of laboratory consolidation using the SHANSEP procedure.

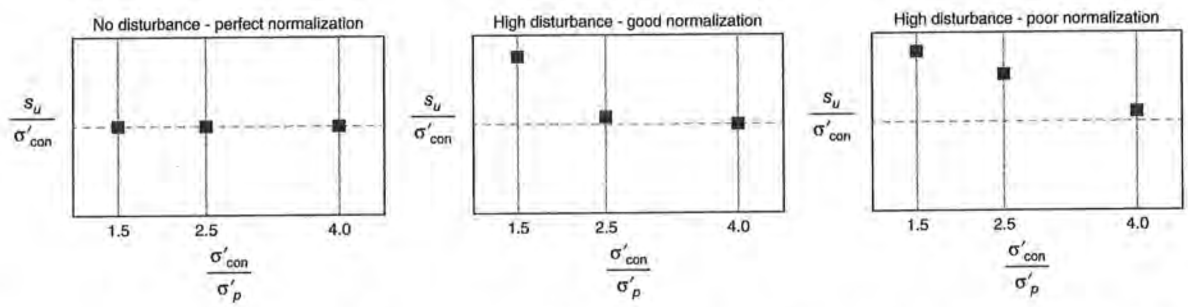

Figure 5.43 Hypothetical plots of undrained strength ratio versus stress ratio to determine degree of disturbance and normalization.

The first plot shows a soil that exhibits no effect of disturbance and perfect normalized behavior. The same undrained strength ratio is obtained for all consolidation stresses. The second plot shows a soil that has significant disturbance, but the sample exhibits normalized behavior as the effect of disturbance has been removed with the use of higher consolidation stresses. It is possible to estimate the undrained strength ratio for a case like this where there is little to no disturbance. The third plot shows a sample that exhibits both high disturbance and poor normalization. In such cases it is not possible to estimate an appropriate value of undrained strength ratio.

5.4.5 Typical Peak Effective Stress Friction Angles for Intact Clays

Tests to measure peak effective stress strength parameters (c' and ϕ') of clays include consolidated–drained direct shear tests (ASTM D3080, 2011) and consolidated–undrained triaxial tests (ASTM D4767, 2011). The laboratory tests should be performed on undisturbed test specimens. Consolidated–drained triaxial tests (ASTM D7181, 2011) can also be used to measure drained strength parameters, but these tests often take a very long time, owing to the low permeability of clay, and thus are usually not practically useful.

Typical values of ϕ' for normally consolidated clays are given in Table 5.16. Strength envelopes for normally consolidated clays go through the origin of stresses, and $c' = 0$ for these materials.

If the clay exhibits inherent anisotropy, as is often the case with lacustrine and riverine deposits, then triaxial tests and direct shear tests may provide different drained friction angles. If the soil deposit has horizontal layering, then lower friction angles may be measured using direct shear tests where the failure plane is horizontal, than in triaxial tests, where the shear plane is inclined. Figure 5.44 shows results from CU triaxial tests and CD direct shear tests conducted

Technically Complete, March 11, 2016

Table 5.16 Typical Values of Peak Friction Angle (ϕ') for Normally Consolidated Clays[a]

Plasticity Index	ϕ' (deg)
10	33 ± 5
20	31 ± 5
30	29 ± 5
40	27 ± 5
60	24 ± 5
80	22 ± 5

[a] $c' = 0$ for these materials.
Source: Data from Bjerrum and Simons (1960).

on normally consolidated clays from southeast Louisiana. It is clear that the triaxial test produced higher friction angles than the direct shear test.

5.4.6 Stiff-Fissured Clays

Heavily overconsolidated clays are usually stiff, and they usually contain fissures. The term *stiff-fissured clays* is often used to describe them. Terzaghi (1936) pointed out what has since been confirmed by many others—the strengths that can be mobilized in stiff-fissured clays in the field are less than the strength of the same material measured in the laboratory.

Skempton (1964, 1970, 1977, 1985), Bjerrum (1967), and others have shown that this discrepancy is due to swelling and softening that occurs in the field over long periods of time but does not occur in the laboratory within the period of time used to perform laboratory strength tests. A related factor is that fissures, which have an important effect on the strength of the clay in the field, are not properly represented in laboratory samples unless the test specimens are large enough to include a representative number of fissures. Unless the specimen size is several times the average fissure spacing, both drained and undrained strengths measured in laboratory tests will be too high.

Peak, Fully Softened, and Residual Strengths of Stiff-Fissured Clays Skempton (1964, 1970, 1977, 1985) investigated a number of slope failures in the stiff-fissured London Clay and developed procedures for evaluating the drained strengths of stiff-fissured clays that have now been widely accepted. Figure 5.45 shows stress–displacement curves and strength envelopes for drained direct shear tests on stiff-fissured clays. The undisturbed peak strength is the strength of undisturbed test specimens from the field. The magnitude of the cohesion intercept (c') depends on the size of the test specimens. Generally, the larger the test specimens, the smaller the value of c'. As displacement continues beyond the peak, reached at $\Delta x = 0.1$ to 0.25 in., the shearing resistance decreases. At displacements of 10 in. or so, the shearing resistance decreases to a residual value. In clays without coarse particles, the decline to residual strength is accompanied by formation of a slickensided surface along the shear plane.

If the same clay is remolded, mixed with enough water to raise its water content to the Liquid Limit, consolidated in the shear box, and then tested, its peak strength will be lower than the undisturbed peak. The strength after remolding and reconsolidating is shown by the NC (normally consolidated) stress–displacement curve and shear strength envelope. The peak is less pronounced, and the NC strength envelope passes through the origin, with c' equal to zero. As shearing displacement increases, the shearing resistance decreases to the same residual value as in the test on the undisturbed test specimen. The displacement required to reach the residual shearing resistance is again about 10 in.

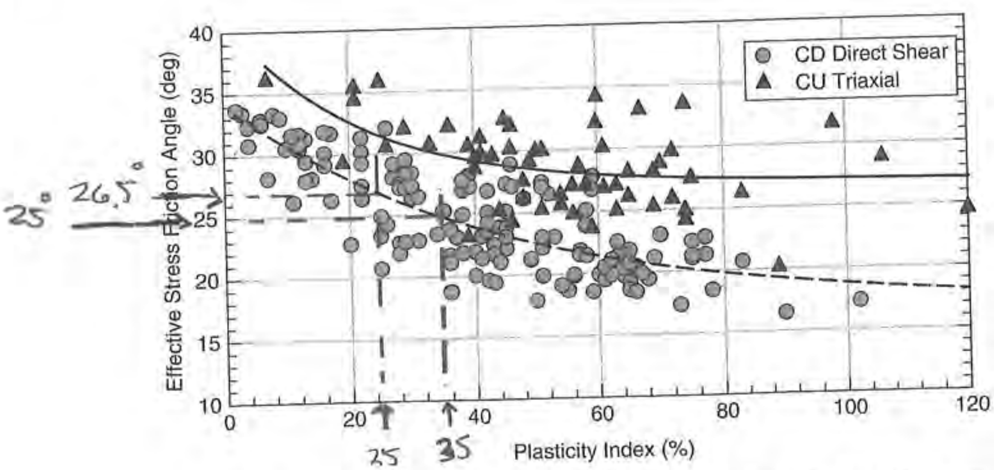

Figure 5.44 Friction angles determined using CU triaxial and CD direct shear tests on southeast Louisiana alluvial clays.

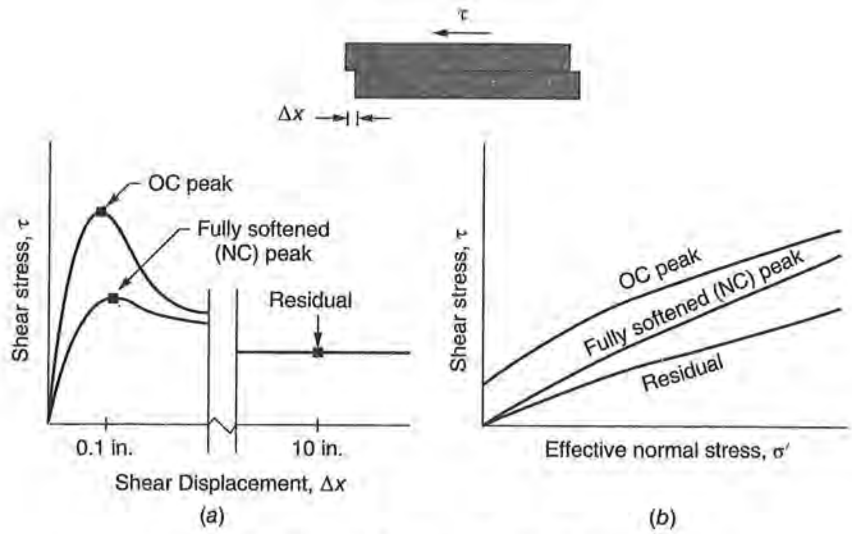

Figure 5.45 Drained shear strength of stiff-fissured clay.

Studies by Terzaghi (1936), Henkel (1957), Skempton (1964), Bjerrum (1967), and others have shown that factors of safety calculated using undisturbed peak strengths for slopes in stiff-fissured clays are larger than unity for slopes that have failed. It is clear, therefore, that laboratory tests on undisturbed test specimens of stiff-fissured clays do not result in strengths that can be used to evaluate the stability of slopes in the field.

Skempton (1970) suggested that this discrepancy is due to the fact that more swelling and softening occur in the field than in the laboratory. He showed that the NC peak strength, also called the *fully softened strength*, corresponds well to strengths back-calculated from *first-time slides*, slides that occur where there is no preexisting slickensided failure surface. Skempton also showed that once a failure has occurred and a continuous slickensided failure surface has developed, only the residual shear strength is available to resist sliding. Tests to measure fully softened and residual drained strengths of stiff clays can be performed using any representative sample, disturbed or undisturbed, because they are performed on remolded test specimens.

Direct shear tests have been used to measure fully softened and residual strengths. They are more suitable for measuring fully softened strengths because the displacement required to mobilize the fully softened peak strength is small, usually about 0.1 to 0.25 in. Direct shear tests are not so suitable for measuring residual strengths because it is necessary to displace the top of the shear box back and forth to accumulate sufficient displacement to develop a slickensided surface on the shear plane and reduce the shear strength to its residual value. Ring shear tests (Stark and Eid, 1993; Bromhead, 1979) are preferable for measuring residual shear strengths because unlimited shear displacement is possible through continuous rotation. Ring shear tests have also been used to measure fully softened shear strengths. An ASTM standard (D7608, 2010) is available to provide guidance for using this apparatus for measuring fully softened shear strength.

Figures 5.46 and 5.47 show correlations of fully softened friction angle and residual friction angle with Liquid Limit, clay size fraction, and effective normal stress. These correlations were developed by Stark and Hussain (2013). Both fully softened and residual friction angles are fundamental soil properties, and the correlations shown in Figures 5.45 and 5.46 have little scatter. Effective normal stress is a factor because the fully softened and residual strength envelopes are curved, as are the strength envelopes for granular materials. It is thus necessary to represent these strengths using nonlinear relationships between shear strength and normal stress, or to select values of ϕ' that are appropriate for the range of effective stresses in the conditions analyzed.

Undrained Strengths of Stiff-Fissured Clays The undrained strength of stiff-fissured clays is also affected by fissures. Peterson et al. (1957) and Wright and Duncan (1972) showed that the undrained strengths of stiff-fissured clays and shales decreased as test specimen size increased. Small specimens are likely to be intact, with few or no fissures, and therefore stronger than a representative mass of the fissured clay. Heavily overconsolidated stiff-fissured clays and shales are also highly anisotropic. As shown in Figure 5.22, the strengths of inclined specimens of Pepper shale and Bearpaw shale, where failure occurs on horizontal planes, are only 30 to 40 percent of the strengths of vertical specimens.

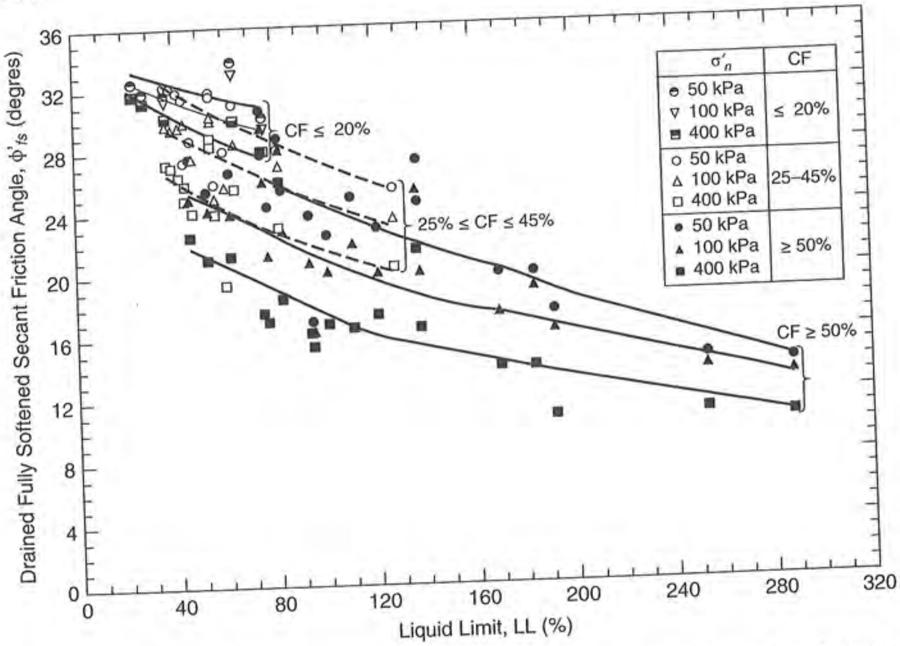

Figure 5.46 Correlation among Liquid Limit, clay size fraction, and fully softened friction angle (Stark and Hussain, 2013). Reproduced with permission from the American Society of Civil Engineers.

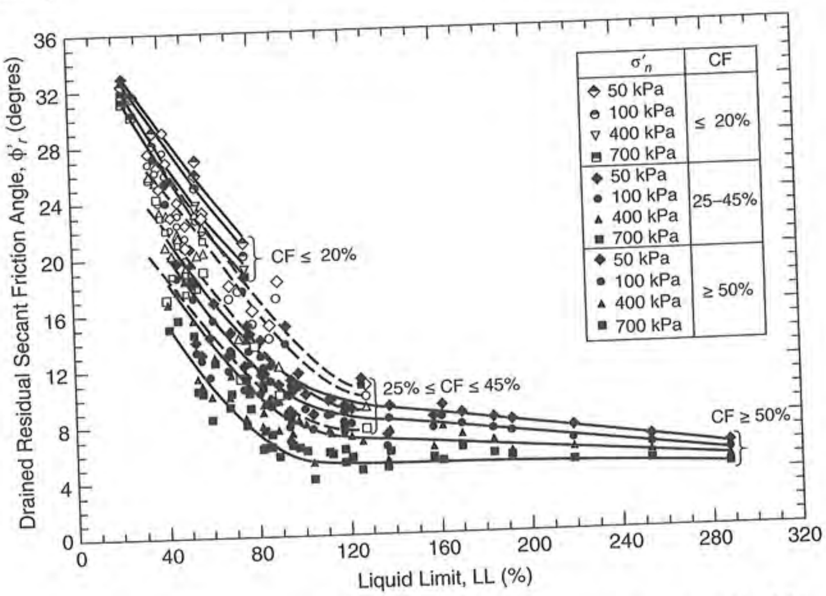

Figure 5.47 Correlation among Liquid Limit, clay size fraction, and residual friction angle (Stark and Hussain, 2013). Reproduced with permission from the American Society of Civil Engineers.

5.4.7 Compacted Clays

Compacted clays are used often to construct embankment dams, highway embankments, and fills to support buildings. When compacted well, at suitable water content, clay fills have high strength. Clays are more difficult to compact than are cohesionless fills. It is necessary to maintain their moisture contents during compaction within a narrow range to achieve good compaction, and more equipment passes are needed to produce high-quality fills. High pore pressures can develop in fills that are compacted wet of optimum, and stability during construction can be a problem in wet fills.

Long-term stability can also be a problem, particularly with highly plastic clays, which are subject to swell and strength loss over time. It is necessary to consider both short- and long-term stability of compacted fill slopes in clay.

Compacted clays are partially saturated soils since occluded air bubbles are not removed by the compaction process. As discussed in Chapter 3, alternative theories have been developed that address the calculation of effective stress and the determination of shear strengths for partially saturated soil. Although these theories are incorporated into many commercial slope stability programs, their use is not common in conventional engineering practice. The equipment needed to determine the necessary strength parameters is not found in many commercial laboratories and the test procedures have not been well standardized. The procedures considered here for compacted clay, and other partially saturated soils, are accepted in conventional geotechnical engineering practice and do not incorporate partially saturated soil mechanics.

Drained Strengths of Compacted Clays Values of c' and ϕ' for compacted clays can be measured using the same laboratory methods as used for intact clays (CD direct shear and CU triaxial with pore pressure measurement). However, conducting triaxial tests on compacted clays is more demanding because compacted clays, especially when compacted dry of optimum, can undergo considerable swell during back pressure saturation. Care is needed to prevent large volume changes prior to applying the final consolidation stress. In addition, CU triaxial test specimens must be fully saturated at the time of shear for accurate pore pressure measurement, and this often requires very high back pressures.

If either direct shear or triaxial tests are properly conducted, the values determined from either type of test are the same for practical purposes. The effective stress strength parameters for compacted clays, measured using samples that have been saturated before testing, are not strongly affected by compaction water content.

Table 5.17 lists typical values of c' and ϕ' for cohesive soils compacted to RC = 100 percent of the standard Proctor maximum dry density. As the value of RC decreases below 100 percent, values of ϕ' remain about the same, and the value of c' decreases. For RC = 90 percent, values of c' are about half the values shown in Table 5.17.

Compacted highly plastic clays can undergo very significant cracking and softening in arid climates. Wright and his colleagues examined shallow slope failures in embankments constructed of Paris and Beaumont Clays in Texas (Staufer and Wright, 1984; Green and Wright, 1986; Rogers and Wright, 1986; Kayyal and Wright, 1991). Laboratory tests on specimens subjected to cycles of drying and wetting to simulate climate cycles showed that the drained strength

Table 5.17 Typical Peak Drained Strengths for Compacted Cohesive Soils

Unified Classification Symbol	Relative compaction, RC[a] (%)	Effective Stress Cohesion, c' (lb/ft^2)	Effective Stress Friction Angle, ϕ' (deg)
SM-SC	100	300	33
SC	100	250	31
ML	100	200	32
CL-ML	100	450	32
CL	100	300	28
MH	100	450	23
CH	100	250	19

[a] RC, relative compaction by USBR standard method, same energy as the standard Proctor (ASTM D698) compaction test.
Source: After U.S. Department of the Interior (1973).

of these clays was reduced to the fully softened strength after many cycles. The fully softened strengths of the highly plastic clays compared well with strengths determined from back analysis of the observed failures, assuming that the piezometric surface was located at the surface of the slope.

Undrained Strengths of Compacted Clays Values of c and ϕ (total stress shear strength parameters) for the as-compacted condition can be determined by performing UU triaxial tests on specimens compacted in the laboratory. Undrained strength envelopes for compacted, partially saturated clays are curved, as discussed in Chapter 3. Over a given range of stresses, however, a curved strength envelope can be approximated by a straight line and can be characterized in terms of c and ϕ. When this is done, it is especially important that the range of pressures used in the tests correspond to the range of pressures in the field conditions being evaluated. Alternatively, if the computer program used accommodates nonlinear strength envelopes, the strength test data can be represented directly.

Values of total stress c and ϕ for compacted clays vary with compaction water content and density. An example is shown in Figure 5.48 for compacted Pittsburg sandy clay. The range of confining pressures used in these tests was 1.0 to 6.0 tons/ft^2. The value of c, the total stress cohesion intercept from UU tests, increases with dry density but is not much affected by compaction water content. The value of ϕ, the total stress friction angle, decreases as compaction water content increases but is not so strongly affected by dry density.

If compacted clays are allowed to age prior to testing, they become stronger, apparently due to thixotropic effects. Therefore, undrained strengths measured using freshly compacted laboratory test specimens provide a conservative

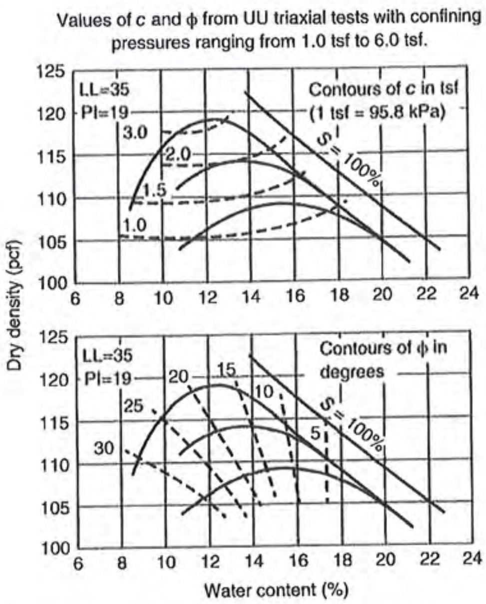

Figure 5.48 Strength parameters for compacted Pittsburg sandy clay tested under UU test conditions (after Kulhawy et al., 1969).

estimate of the strength of the fill a few weeks or months after compaction.

Recapitulation

- The shear strength of clays in terms of effective stress can be expressed by the Mohr–Coulomb strength criterion as $s = c' + \sigma' \tan \phi'$.
- The shear strength of clays in terms of total stress can be expressed as $s = c + \sigma \tan \phi$.
- For saturated clays, ϕ is zero, and the undrained strength can be expressed as $s = s_u = c$, $\phi = \phi_u = 0$.
- Samples used to measure undrained strengths of normally consolidated and moderately overconsolidated clay should be as nearly undisturbed as possible.
- The strengths that can be mobilized in stiff-fissured clays in the field are less than the strength of the same material measured in the laboratory using undisturbed test specimens.
- The normally consolidated peak strength, also called the fully softened strength, corresponds to strengths back-calculated from first-time slides in stiff-fissured clays.
- Once a failure has occurred and a continuous slickensided failure surface has developed, only the residual shear strength is available to resist sliding.
- Tests to measure fully softened and residual drained strengths of stiff clays can be performed on remolded test specimens.
- Ring shear tests are preferable for measuring residual shear strengths because unlimited shear displacement is possible through continuous rotation.
- Values of c' and ϕ' for compacted clays can be measured using consolidated–undrained triaxial tests with pore pressure measurements or consolidated–drained direct shear tests.
- Undrained strengths of compacted clays vary with compaction water content and density and can be measured using UU triaxial tests performed on specimens at their as-compacted water contents and densities.

5.5 MUNICIPAL SOLID WASTE

Waste materials have strengths comparable to the strengths of soils. Strengths of waste materials vary depending on the amounts of soil and sludge in the waste, as compared to the amounts of plastic and other materials that tend to interlock and provide tensile strength (Eid et al., 2000). Larger amounts of materials that interlock increase the strength of the waste. Although solid waste tends to decompose or degrade with time, Kavazanjian (2001) indicates that the strength after degradation is similar to the strength before degradation.

Kavazanjian et al. (1995) used laboratory test data and back analysis of stable slopes to develop the lower-bound strength envelope for municipal solid waste (MSW) shown in Figure 5.49. The envelope is horizontal with a constant strength $c = 24$ kPa, $\phi = 0$ at normal pressures less than 37 kPa. At pressures greater than 37 kPa, the envelope is inclined at $\phi = 33$ degrees, with $c = 0$.

Eid et al. (2000) used results of large-scale direct shear tests (300 to 1500 mm shear boxes) and back analysis of failed

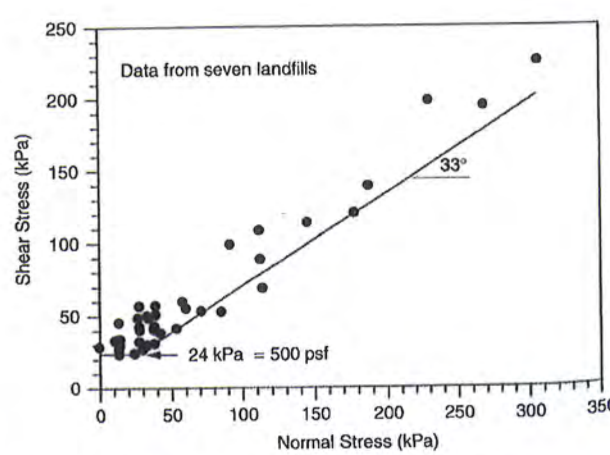

Figure 5.49 Shear strength envelope for municipal solid waste based on large-scale direct shear tests and back analysis of stable slopes (after Kavazanjian et al., 1995).

Reference No. 7

Empirical Correlations Between
Plasticity Indices & Consolidation Parameters

Technically Complete, March 11, 2016

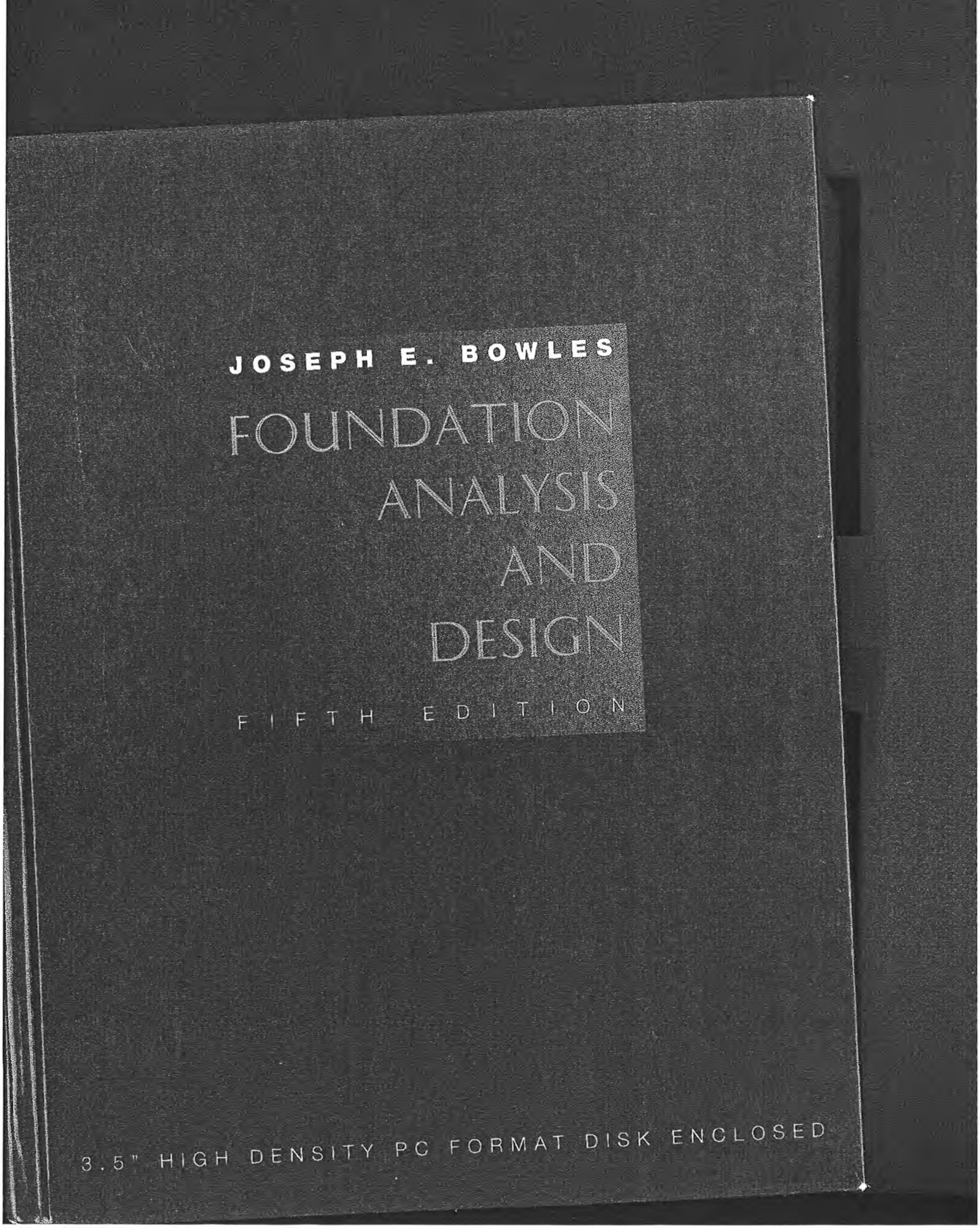

Technically Complete, March 11, 2016

TABLE 2-5
Correlation equations for soil compressibility/consolidation

Compression index, C_c	Comments	Source/Reference
$C_c = 0.009(w_L - 10)$ ($\pm$30% error)	Clays of moderate S_t	Terzaghi and Peck (1967)
$C_c = 0.37(e_o + 0.003w_L + 0.0004w_N - 0.34)$	678 data points	Azzouz et al. (1976)
$C_c = 0.141G_s\left(\frac{\gamma_{sat}}{\gamma_{dry}}\right)^{2.4}$	All clays	Rendon-Herrero (1983)
$C_c = 0.0093w_N$	109 data points	Koppula (1981)
$C_c = -0.0997 + 0.009w_L + 0.0014I_P + 0.0036w_N + 0.1165e_o + 0.0025C_P$	109 data points	Koppula (1981)
$C_c = 0.329[w_N G_s - 0.027w_P + 0.0133I_P(1.192 + C_P/I_P)$	All inorganic clays	Carrier (1985)
$C_c = 0.046 + 0.0104I_P$	Best for $I_P < 50\%$	Nakase et al. (1988)
$C_c = 0.00234w_L G_s$	All inorganic clays	Nagaraj and Srinivasa Murthy (1985, 1986)
$C_c = 1.15(e_o - 0.35)$	All clays	Nishida (1956)
$C_c = 0.009w_N + 0.005w_L$	All clays	Koppula (1986)
$C_c = -0.156 + 0.411e_o + 0.00058w_L$	72 data points	Al-Khafaji and Andersland (1992)
Recompression index, C_r		
$C_r = 0.000463w_L G_s$		Nagaraj and Srinivasa Murthy (1985)
$C_r = 0.00194(I_P - 4.6)$	Best for $I_P < 50\%$	Nakase et al. (1988)
$= 0.05$ to $0.1C_c$	In desperation	
Secondary compression index, C_α		
$C_\alpha = 0.00168 + 0.00033I_P$		Nakase et al. (1988)
$= 0.0001w_N$		NAFAC DM7.1 p. 7.1-237
$C_\alpha = 0.032C_c$	$0.025 < C_\alpha < 0.1$	Mesri and Godlewski (1977)
$= 0.06$ to $0.07C_c$	Peats and organic soil	Mesri (1986)
$= 0.015$ to $0.03C_c$	Sandy clays	Mesri et al. (1990)

Notes: 1. Use w_L, w_P, w_N, I_P as percent, not decimal.
2. One may compute the in situ void ratio as $e_o = w_N G_s$ if $S \to 100$ percent.
3. C_p = percent clay (usually material finer than 0.002 mm).
4. Equations that use e_o, w_N, and w_L are for both normally and overconsolidated soils.

2-10.8 Compression Index Correlations and Preconsolidation

A reliable estimate of the *effective preconsolidation pressure* p'_c is difficult without performing a consolidation test. There have been a few correlations given for p'_c of which one was given by Nagaraj and Srinivasa Murthy (1985, 1986) for saturated soils preconsolidated by overburden pressure (as opposed to shrinkage or chemical factors):

$$\boxed{\log_{10} p'_c = 5.97 - 5.32(w_N/w_L) - 0.25\log_{10} p'_o} \tag{2-50}$$

As an example, for

$$w_N = 25\%; \quad w_L = 50\% \text{ (liquid limit)};$$

$$p'_o = \gamma'_s z = 16 \times 3\text{ m} = 48\text{ kPa}$$

we have

$$\log_{10} p'_c = 5.97 - 5.32(0.25/0.50) - 0.25 \log_{10} 48$$
$$= 2.89 \rightarrow p'_c = 10^{2.89} = \mathbf{776}\ \text{kPa}$$

The OCR = 776/48 = **16**. While this is a very large OCR, we could have predicted that there would be some overconsolidation, with $w_N = w_L/2$—certainly a case where w_N is closer to w_P than to w_L.

For soils preconsolidated by cementation and shrinkage Nagaraj and Srinivasa Murthy (1985, 1986) suggest

$$p'_c = 3.78s_u - 2.9 \text{ (units of kPa)} \tag{2-51}$$

where s_u = in situ undrained shear strength as defined in Sec. 2-11.4 and determined by the field vane shear test described in Sec. 3-12.

As previously noted, it is possible to estimate whether a soil is preconsolidated from overburden pressure by noting the position of the natural water content w_N with respect to the Atterberg limits of w_P and w_L on Fig. 2-2*a*:

1. If w_N is closer to the liquid limit w_L than to w_P the soil is likely to be *normally consolidated.*
2. If w_N is closer to the plastic limit w_P than to w_L the soil is likely to be *preconsolidated.*

Unfortunately this information cannot be used in a quantitative manner or for over- or preconsolidation caused by shrinkage or chemical action. All that can be said with any certainty is that if the soil is preconsolidated it is not likely to settle as much under a foundation load as a similar soil in a normally consolidated state.

2-11 SHEAR STRENGTH

Soil strength is the resistance to mass deformation developed from a combination of particle rolling, sliding, and crushing and is reduced by any pore pressure that exists or develops during particle movement. This resistance to deformation is the shear strength of the soil as opposed to the compressive or tensile strength of other engineering materials. The shear strength is measured in terms of two soil parameters: interparticle attraction or *cohesion* c, and resistance to interparticle slip called the *angle of internal friction* ϕ. Grain crushing, resistance to rolling, and other factors are implicitly included in these two parameters. In equation form the shear strength in terms of *total* stresses is

$$s = c + \sigma \tan \phi \tag{2-52}$$

and, using *effective* strength parameters,

$$s = c' + \sigma' \tan \phi' \tag{2-52a}$$

where terms not identified earlier are

s = shear strength (sometimes called τ), kPa, ksf, etc.

σ = normal stress on shear plane (either total σ or effective σ'), kPa, ksf, etc.

$\sigma' = \sigma - u$ = effective normal stress (defined in Sec. 2-9)

Reference Nos. 8, 9, 10, 11, and 12

Material Properties for Municipal Solid Waste

Technically Complete, March 11, 2016

Available online at www.sciencedirect.com

SCIENCE DIRECT

ELSEVIER

Geotextiles and Geomembranes 23 (2005) 205–233

Geotextiles and Geomembranes

www.elsevier.com/locate/geotexmem

Engineering properties of municipal solid waste

Neil Dixon[a,*], D. Russell V. Jones[b]

[a] *Department of Civil and Building Engineering, Loughborough University, Leicestershire, LE11 3TU, UK*
[b] *Golder Associates (UK) Ltd, Attenborough House, Browns Lane Business Park, Stanton-on-the-Wolds, Nottinghamshire, NG12 5BL, UK*

Received 3 February 2004; received in revised form 24 November 2004; accepted 26 November 2004

Abstract

Mechanical behaviour of the waste body controls many aspects of landfill lining system design and performance, including stability issues and integrity of the geosynthetic and mineral lining components. Knowledge of the likely ranges of waste mechanical properties is required to assess potential modes of failure and hence to design the landfill engineering measures. This paper provides a summary of measurement and interpretation issues for the key engineering parameters used to define: unit weight, compressibility, shear strength, lateral stiffness, in situ horizontal stress and hydraulic conductivity. The topic of waste mechanics is developing rapidly and many papers have been published on waste mechanics, reporting results from both laboratory and in situ studies. Although waste is heterogeneous, many of the studies show that municipal solid waste has mechanical properties that vary in a consistent and predictable way (e.g. with respect to stress state and method of placement). An internationally agreed classification system and test standards are required to allow interpretation of published results. This will lead to development of appropriate constitutive models for waste and hence to optimization of landfill designs by considering waste/lining system interaction in full.

Keywords: Landfill engineering; Waste mechanics; Lining systems

*Corresponding author. Tel.: +1440 1509 228542; fax: +1440 1509 223945.
E-mail addresses: n.dixon@lboro.ac.uk (N. Dixon), RJones@golder.com (D.R.V. Jones).

0266-1144/$ - see front matter © 2005 Elsevier Ltd. All rights reserved.
doi:10.1016/j.geotexmem.2004.11.002

Technically Complete, March 11, 2016

changes in size and alteration of the mechanical properties (i.e. compressibility and shear strength). It will also change the density of the component. As a waste body degrades, void ratio reduces and hence a volume reduction occurs. Although there are few field measurements in degraded waste it is generally believed that degradation results in an increase in waste density, and hence unit weight.

2.4. Compaction

Since MSW is a particulate material and a large proportion of the components have a high void ratio and a high compressibility, compaction processes will reduce the voids within an individual component as well as voids between various components. The unit weight of compacted waste will depend upon the waste components, thickness of layer, weight and type of compaction plant and the number of times equipment passes over the waste. A layer thickness of 0.5–1.0 m will facilitate the achievement of good compaction and hence high unit weights, however it is not untypical for waste to be placed in layers of 2–3 m thick. This results in poor-to-moderate compaction. Fassett et al. (1994) conducted a detailed survey of bulk unit weight data from the international literature. A statistical analysis of the data is shown in Table 4. The degree of compaction was derived from an assessment of individual site practices. Poor relates to little or no compaction, moderate to 'old' practices and good to 'current' (1994) practices. The assessment was in most cases subjective but provides a useful guide. An important result is the large variation in unit weight when little or no compaction is used. Landva and Clark (1990) and Oweis and Khera (1986) report similar ranges of bulk unit weights. A summary of measured values from recent studies conducted in four countries is provided in Table 5. These are also consistent with the Fassett et al. (1994) reported values and indicate that current practice is still only achieving 'moderate' levels of compaction for placement of fresh MSW.

2.5. Depth

Unit weight of waste varies with effective stress, which is a function of depth. Fig. 3 produced by Powrie and Beaven (1999) shows the variation in dry density, saturated density and density at field capacity with vertical effective stress. The data was obtained by compressing samples of waste in a large diameter cylindrical tests

Table 4
Statistical summaries of bulk unit weight data for fresh waste (Fassett et al., 1994)

	Poor compaction	Moderate compaction	Good compaction
Range (kN/m^3)	3.0–9.0	$\boxed{5.0–7.8}$ 32–50pcf	8.8–10.5
Average (kN/m^3)	5.3	7.0	9.6
Standard deviation (kN/m^3)	2.5	0.5	0.8
Coefficient of variation (%)	48	8	8

Unit Weight of Municipal Solid Waste

Dimitrios Zekkos, A.M.ASCE[1]; Jonathan D. Bray, M.ASCE[2]; Edward Kavazanjian Jr., M.ASCE[3]; Neven Matasovic, M.ASCE[4]; Ellen M. Rathje, M.ASCE[5]; Michael F. Riemer, M.ASCE[6]; and Kenneth H. Stokoe II, M.ASCE[7]

Abstract: The unit weight of municipal solid waste (MSW) is an important parameter in engineering analyses of landfill performance, but significant uncertainty currently exists regarding its value. A careful review of reliable field data shows that individual landfills have a characteristic MSW unit weight profile. Based on in situ unit weight data and trends observed in large-scale laboratory tests, a hyperbolic relationship was developed to represent this characteristic MSW unit weight profile. Within the context of this characteristic profile, landfill-specific values of MSW unit weight depend primarily on waste composition, operational practices (i.e., compaction, cover soil placement, and liquids management), and confining stress. Guidance is provided for developing landfill-specific MSW unit weight profiles, including procedures for performing large-scale tests for in situ measurement of MSW unit weight at a landfill.

DOI: 10.1061/(ASCE)1090-0241(2006)132:10(1250)

CE Database subject headings: Municipal wastes; Landfills; Density; Waste sites; Weight; Waste management.

Introduction

The unit weight of municipal solid waste (MSW) is an important material property in landfill engineering. MSW unit weight is required for many engineering analyses of landfill systems, including static and dynamic slope stability, geomembrane puncture, pipe crushing, and landfill capacity evaluation. However, the value of the unit weight of MSW continues to be a major source of uncertainty in landfill performance analyses. Significant scatter exists in the reported values of MSW unit weight. Hence, it is difficult for an engineer to estimate with confidence a representative MSW unit weight profile for use in engineering analyses.

Significantly different MSW unit weight profiles have been reported in the literature. The TC5-Environmental Geotechnics Committee report (Konig and Jessberger 1997), citing the data of Fassett (1993) and other researchers, reports unit weight values from 3 kN/m^3 for uncompacted or poorly compacted waste to 17 kN/m^3 for compacted waste. As compiled by Zekkos et al. (2005b), values of in-place MSW unit weight reported at 37 different landfills varied from 3 to 20 kN/m^3. The majority of these studies do not report the method used to establish the MSW unit weight. Landva and Clark (1986) presented results from in situ near-surface test pits in several Canadian landfills and emphasized the difference between the unit weights of refuse, soil cover, and combinations of the two. The total unit weight near the landfill surface of combinations of refuse and soil cover estimated from the data reported by Landva and Clark (1986) ranged from 8 to 17 kN/m^3. Presumably, the values cited by the other researchers also represent the total unit weight of the refuse/soil cover mixture, as this is the parameter of relevance for engineering analysis. This combined refuse/soil unit weight is referred to throughout this paper as MSW unit weight.

The MSW unit weight profile of Kavazanjian et al. (1995) is one of the most commonly cited MSW unit weight profiles in the literature (even though the lead author has revised it several times since then). This profile starts from a value of about 6 kN/m^3 near the surface and reaches a value of about 13 kN/m^3 at depths of 45 m or larger. It was developed primarily based upon values reported by landfill operators for relatively dry landfills, i.e., landfills conforming to U.S. EPA restrictions against the introduction of liquids. However, subsequent studies indicated that, even for dry landfills, the unit weight values in the 1995 profile were relatively low. Kavazanjian (1999) explains that "in developing the [1995] curve, it was assumed that the operator reported values of unit weight represented the total unit weight of soil and refuse when, in fact, they represented only the weight of the refuse in a unit volume of landfill." Therefore, in subsequent work, this 1995 profile was adjusted upwards to account for the daily and interim cover soil typically placed in the landfill over the waste. Kavazanjian et al. (1996) report MSW unit weight values from 10 to 13 kN/m^3 near the ground surface increasing to 13–16 kN/m^3 at a depth of 30 m at six California landfills, based upon correlation with shear wave velocity measurements. Kavazanjian (1999) shows a "typical" unit weight profile with minus and plus one standard deviation bounds (based upon correlation with shear

[1]Senior Staff Engineer, GeoSyntec Consultants, 475 14th St., Suite 450, Oakland, CA 94612.

[2]Professor, Dept. of Civil and Environmental Engineering, Univ. of California, Berkeley, CA 94720.

[3]Associate Professor, Dept. of Civil and Environmental Engineering, Arizona State Univ., Tempe, AZ 85287.

[4]Associate, GeoSyntec Consultants, 2100 Main St., Suite 150, Huntington Beach, CA 92648.

[5]Associate Professor, Dept. of Civil, Architectural and Environmental Engineering, Univ. of Texas at Austin, Austin, TX 78712.

[6]Adjunct Professor, Dept. of Civil and Environmental Engineering, Univ. of California at Berkeley, Berkeley, CA 94720.

[7]Professor, Dept. of Civil, Architectural and Environmental Engineering, Univ. of Texas at Austin, Austin, TX 78712.

Note. Discussion open until March 1, 2007. Separate discussions must be submitted for individual papers. To extend the closing date by one month, a written request must be filed with the ASCE Managing Editor. The manuscript for this paper was submitted for review and possible publication on August 16, 2005; approved on May 3, 2006. This paper is part of the ***Journal of Geotechnical and Geoenvironmental Engineering***, Vol. 132, No. 10, October 1, 2006. ©ASCE, ISSN 1090-0241/2006/10-1250–1261/$25.00.

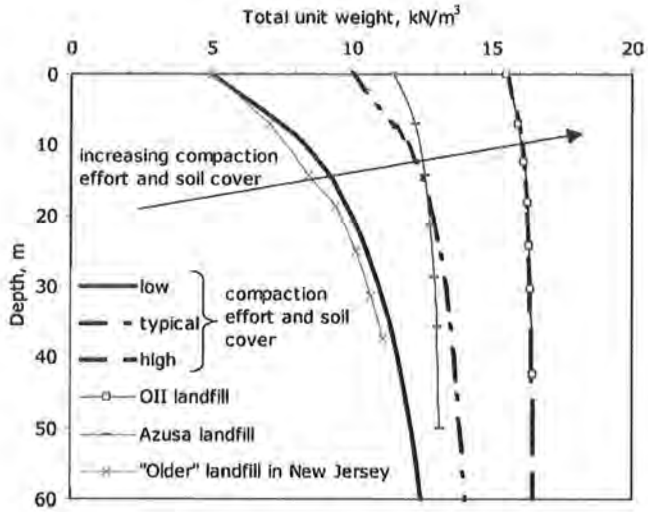

Fig. 11. Recommended unit weight profiles for conventional municipal solid-waste landfills. The near-surface in-place unit weight depends on waste composition (including moisture content) in addition to compaction effort and the amount of soil cover. The effect of confining stress is represented by depth.

MSW Unit Weight Model

The model described by Eq. (4) was fit to the field data presented in Fig. 3. The fitted hyperbolas are shown in Fig. 3 as solid lines for each landfill. In the fitting process, the near-surface in-place unit weight was assigned based upon the field data and then the hyperbolic parameters β and α were estimated based upon a visual "best fit" to the data.

Fig. 11 illustrates a family of representative MSW unit weight profiles developed using this model. Model parameters for the three representative profiles shown in Fig. 11 (for low, typical, and high near-surface in-place unit weight) are provided in Table 2. The in-place near-surface MSW unit weight for a particular waste material primarily increases with compaction effort and soil content and the increase in unit weight with confining stress at depth becomes less pronounced with increasing near-surface in-place unit weight (moving from the continuous curve on the left-hand side toward the dashed curve to the right-hand side). The recommended curves are supported by the field-fitted hyperbolas, some of which are shown in this figure, and the laboratory test data described previously.

Moisture content is not explicitly included in the MSW unit weight model because for conventional landfills it was found to be of lesser importance and was not measured consistently in the field studies of MSW unit weight. Reliable moisture content measurements ranged from approximately 10%–50%. The curves shown in Fig. 11 are considered reasonable for typical conventional landfills, i.e., landfills with moisture contents at or below field capacity. The moisture content of the waste, although not explicitly included in Fig. 11, may affect where, within the family of typical unit weight profiles, a particular landfill falls, i.e., an increase in moisture content will move the representative unit weight curve for a given landfill to the right in Fig. 11.

Table 2. Hyperbolic Parameters for Different Compaction Effort and Amount of Soil Cover

Compaction effort and soil amount	γ_i (kN/m^3)	β (m^3/kN)	α (m^4/kN)
Low	5	0.1	2
Typical	10	0.2	3
High	15.5	0.9	6

Waste compressibility, as represented by the modified compression indices, $C_{c\varepsilon}$, can be estimated from the recommended unit weight curves for low, typical, and high in-place near-surface unit weight. Defining the modified compression index $C_{c\varepsilon}$ as the slope of the volumetric strain-log vertical stress plot and assuming no loss of mass (no degradation), it can be shown that for material that has a total unit weight of γ_{t1} at an initial vertical effective stress σ'_{v1} and a total unit weight of γ_{t2} at vertical effective stress σ'_{v2}, the equivalent modified compression index is given by the following equation:

$$C_{c\varepsilon} = \frac{\Delta e}{1+e_0}\frac{1}{\log\left(\frac{\sigma'_{v1}}{\sigma'_{v2}}\right)} = \frac{\gamma_{t2}-\gamma_{t1}}{\gamma_{t2}}\frac{1}{\log\left(\frac{\sigma'_{v1}}{\sigma'_{v2}}\right)} \tag{5}$$

Using Eq. (5) and discretizing the three recommended unit weight profiles at different depth intervals, values of the MSW equivalent compression index $C_{c\varepsilon}$ that correspond to the representative unit weight profiles in Fig. 11 can be estimated. Using this approach, the resulting $C_{c\varepsilon}$ values are 0.015–0.04, 0.13–0.22, and 0.36–0.55 for high, typical, and low near-surface in-place unit weight, respectively. These values are consistent with previous recommendations on the compressibility of MSW (e.g.,Sowers 1973; Fassett 1993; Kavazanjian et al. 1999).

The parameters of the hyperbolas fitted to the field unit weight data of Fig. 3 are plotted in Fig. 12 to illustrate the relationship of the near-surface in-place unit weight, γ_i, with the β parameter (Chart 1) and the relationship of β with the α parameter (Chart 2). The majority of the field data are in the lower left-hand side of the charts (low initial unit weight, small β and α), with the denser OII Landfill data being in the upper-right portion of these charts due to its large initial unit weight and small difference between its initial unit weight and unit weight at depth. It is reasonable to expect that as the amount of daily soil cover, moisture content, or compaction effort increases, the unit weight near the surface, γ_i, and the α and the β parameters will also increase. As explained previously, the larger the β parameter, the smaller the difference between the unit weight at the surface and at depth, and the larger the α parameter, the smaller the increase of the unit weight near the surface (see Fig. 10).

The field data suggest that γ_i, α, and β increase as the amount of cover-soil or compaction effort increases. This observation is supported by the results of the large-scale triaxial laboratory data shown in Fig. 5. Because the laboratory unit weight data is for isotropic stress conditions, "equivalent" field depths were estimated by calculating the depth at which the isotropic stress in the laboratory is equal to the mean field stress under K_0 ("at rest") stress conditions. A value of K_0 equal to 0.5 was assumed, which is consistent with Poisson's ratio values measured in the triaxial tests for specimens with 100% of the constituents smaller than 20 mm. The laboratory data in Fig. 5 were fit to Eq. (4) and values of γ_i, α, and β, were derived. The resulting values of α and β are shown in Fig. 12 for the Tri-Cities Landfill A3 sample group specimens. Specimen A3-3L included 100% less than 20 mm material and was prepared without compaction. Specimen A3-1L included the same material but was compacted with more effort than specimen A3-3L. Comparison of the parameters de-

The Impact of Degradation on MSW Shear Strength

Edward Kavazanjian, Jr.[1], M. ASCE

[1]Associate Professor, Department of Civil and Environmental Engineering, Arizona State University, Tempe, AZ 85287-5306 edkavy@asu.edu

ABSTRACT: Multiple lines of evidence are used to draw conclusions concerning the shear strength of degraded municipal solid waste (MSW). Interpretation of the accumulated evidence leads to the conclusion that for conventional "dry" landfills the shear strength envelopes commonly used in practice provide reasonable strength values for circular and non-horizontal failure surfaces even for old landfills where the waste may be in a relatively advanced state of degradation. However, for horizontal failure surfaces in conventional landfills that may not engage the fibrous waste components, for landfills where mechanical pre-processing has been used to reduce waste constituent size and facilitate degradation, and for bioreactor landfills, a strength envelope characterized by zero cohesion and an effective friction angle of 30 degrees appears to provide a conservative representation of degraded MSW shear strength.

INTRODUCTION

The impact of degradation on the shear strength of municipal solid waste (MSW) is an important consideration in the landfill design. Concerns that degradation reduces the shear strength of MSW must be addressed when considering the long term stability of a conventional landfill. Furthermore, degraded MSW shear strength may govern both short and long term stability of bioreactor landfills. Recent studies suggesting that the degraded shear strength of MSW may be lower than the shear strengths typically employed in landfill design practice give cause for a critical revaluation of available data on the shear strength of degraded MSW.

MSW SHEAR STRENGTH ENVELOPES USED IN PRACTICE

Two of the most common MSW shear strength envelopes used in practice are the envelopes recommended by Kavazanjian et al. (1995) and Eid et al. (2000). Kavazanjian et al. (1995) recommended a MSW shear strength envelope represented by a cohesion of 24 kPa at low normal stresses and by a friction angle of 33 degrees at high normal stresses. Eid at al. (2000) provided lower bound, median, and upper bound recommendations for MSW shear strength. The lower bound envelope was using the mobilized shear strength at an axial strain of 9% in one isotropically consolidated test and one test consolidated such that the ratio of the horizontal effective stress to vertical effective stress at the end of consolidation (K) was 0.65. This interpretation leads to an effective stress strength represented by an effective cohesion of 22 kPa and an effective friction angle of 20 degrees. If only the result of the test with K=0.65 is used, a secant friction angle on the order of 42 degrees is calculated from the Harris et al. (2006) data for a mean effective normal stress of approximately 60 kPa. Furthermore, results from a test with K=0.29, not employed by Harris et al. (2006) in developing their TC shear strength envelope, yield a secant friction angle of between 46 and 56 degrees for a mean effective normal stress of between 100 and 140 kPa. As discussed previously, Zekkos et al. (2007b) recommend interpreting shear strength from triaxial test data based upon K=0.3.

CONCLUSIONS

The multiple lines of evidence discussed above can be employed to draw conclusions on the shear strength of degraded MSW. Strength envelopes from Kavazanjian et al. (1995) and Eid et al. (2000), developed in part from back analyses of stable and failed landfill slopes, suggest that a friction angle of 33 degrees is adequate to characterize the shear strength of degraded MSW in conventional landfills. Back analysis of the failures of the Doña Juana and Payatas Landfill suggest that a friction angle of at least 30 degrees may adequately describe the shear strength of degraded MSW up to effective normal stresses of 600 kPa. Drained direct shear tests on unprocessed waste from a bioreactor yield a friction angle of 39 degrees for normal stresses of up to 430 kPa. Triaxial tests conducted by Zekkos et al. (2007b) on waste with all >20 mm material removed suggest secant friction angles in excess of 35 degrees for degraded waste for effective confining pressures of up to 200 kPa. A very conservative reinterpretation of direct simple shear tests on processed degraded waste from both a bioreactor landfill and a landfill where the waste was below the water table yield secant friction angles of 26 to 34 degrees for effective normal stresses of up to 700 kPa. Reinterpretation of this triaxial data yields secant friction angles of 42 degrees or greater at effective confining pressures of up to 140 kPa.

Based upon the above-cited evidence, the following recommendations are made concerning the shear strength of degraded MSW for normal stresses of up to 600 kPa. For conventional "dry" landfills, where some fibrous waste should still remain after degradation, shear strength envelopes commonly used in practice provide reasonable strength values for circular and non-horizontal failure surfaces, even for old landfills where the waste may be in a relatively advanced state of degradation. However, for horizontal failure surfaces in conventional landfills, i.e. failure surfaces that may not engage the fibrous waste components, for landfills where pre-processing has been used to reduce waste constituent size and facilitate degradation, and for bioreactor landfills, an effective stress strength envelope characterized by zero cohesion and a friction angle of 30 degrees may be an appropriate conservative representation of the shear strength until further data is available.

Technically Complete, March 11, 2016

Municipal Solid Waste Landfill Settlement: Postclosure Perspectives

Hari D. Sharma, F.ASCE[1]; and Anirban De, M.ASCE[2]

Abstract: This paper presents settlement mechanisms and the methods for estimating settlements of municipal solid waste landfills, including bioreactor landfills. Based on results of field monitoring and data in published literature, coefficients of secondary compression for solid waste due to self-weight and external load are estimated. Special considerations are given to bioreactor landfills. Uses of these coefficients for long-term settlement estimation and their application to postclosure maintenance and development plans are discussed. Four case histories illustrating the use of these coefficients are presented. Methods of landfill treatment to reduce settlements are also presented.

DOI: 10.1061/(ASCE)1090-0241(2007)133:6(619)

CE Database subject headings: Solid wastes; Municipal wastes; Landfills; Waste management.

Introduction

The composition of waste, both in the municipal solid waste (MSW) and hazardous waste landfills, is heterogeneous. According to the Code of Federal Regulations 257.2 a MSW landfill may receive household waste and any other type of Resource Conservation and Recovery Act Subtitle D waste, such as, commercial solid waste, nonhazardous sludge, and industrial solid waste. Data regarding the composition of MSW, collected from actual landfills are presented by Bouazza et al. (1996) and Sharma (2000). The very heterogeneous nature of MSW makes the estimation and prediction of landfill settlement difficult.

Increasing pressure of new development on available real estate is leading to a worldwide trend to construct over former landfill sites. This, in turn, is making it imperative to obtain reasonably accurate predictions of landfill settlements, as design inputs for structures proposed at the site.

Methods of Settlement Estimation

Processes Responsible for Waste Settlement

The mechanism of waste settlement is complex and can be attributed to the following main processes (Sowers 1973; Edil et al. 1990; Sharma and Reddy 2004):

1. Physical and mechanical processes: These include the reorientation of particles, movement of the fine materials into larger voids, and collapse of void spaces.
2. Chemical (physicochemical) process: This includes corrosion, combustion, and oxidation.
3. Dissolution process: This consists of dissolving soluble substances by percolating liquids and then forming leachate.
4. Biological decomposition (biochemical decay): The organics in the refuse will decompose with time, controlled by temperature, humidity, and percentage of organics and nutrients in the waste.

Settlement Estimation Methods for MSW Landfills

Numerous settlement estimation methods for MSW have been proposed in the literature (Sowers 1973; Dodt et al. 1987; Edil et al. 1990, Ling et al. 1998; Park et al. 2002). Brief discussions of some of the more significant methods are presented below.

Sowers Method

Sowers (1973) used equations similar to those used for primary and secondary consolidation of soils to estimate settlements of waste landfills. Total settlement (ΔH) is divided into primary (short-term) settlement (ΔH_p) and secondary or long-term settlement (ΔH_s). The following equations are used to estimate the settlement

$$\Delta H = \Delta H_p + \Delta H_s \quad (1)$$

$$\boxed{\Delta H_p = HC_{ce} \log \frac{p_0 + \Delta p}{p_0}} \quad (2)$$

$$\Delta H_s = H_1 C_\alpha \log \frac{t_2}{t_1} \quad (3)$$

where, H=initial thickness of waste (before load placement); H_1=thickness of waste at the beginning of the secondary settlement (i.e., thickness at $t=t_1$); $C_{ce}=C_c/(1+e_0)$, where C_c=compression index and e_0=void ratio; C_α=secondary com-

[1]Principal, GeoSyntec Consultants, 475 14th St., Suite 450, Oakland, CA 94612.

[2]Assistant Professor, Dept. of Civil & Environmental Engineering, Manhattan College, Bronx, NY 10471.

Note. Discussion open until November 1, 2007. Separate discussions must be submitted for individual papers. To extend the closing date by one month, a written request must be filed with the ASCE Managing Editor. The manuscript for this paper was submitted for review and possible publication on May 4, 2004; approved on September 27, 2006. This paper is part of the ***Journal of Geotechnical and Geoenvironmental Engineering***, Vol. 133, No. 6, June 1, 2007. ©ASCE, ISSN 1090-0241/2007/6-619–629/$25.00.

pression index; p_0=initial overburden pressure; Δp=incremental pressure; t_1=starting time for secondary compression; and t_2=ending time for secondary compression.

Rheological Model

Edil et al. (1990) proposed a method based on the rheological model of Gibson and Lo (1961) to estimate total settlement (ΔH) based on the following equation:

$$\Delta H = H(\Delta p)[a + b\{1 - \exp(-\lambda/b)t\}] \tag{4}$$

where H=initial height of waste; Δp=change in pressure; a=primary compression parameter; b=secondary compression parameter; λ/b=rate of secondary compression, and t=time since load application.

Power Creep Model

The power creep model, as proposed by Edil et al. (1990), uses the following:

$$\Delta H = H\Delta pm(t/t_r)^n \tag{5}$$

expression for settlement (ΔH) estimation where H and Δp are as defined earlier; m=reference compressibility; n=compression rate; t_r=reference time; and t=time since load application.

Hyperbolic Function Model

Ling et al. (1998) applied the hyperbolic function to predict long-term settlements at three landfill sites. They used the following expression to relate settlement with time:

$$S = \frac{t}{1/\rho_0 + t/S_{\text{ult}}} \tag{6}$$

where t=time interval of interest; S=settlement occurring in time interval, t; ρ_0=rate of settlement at the beginning of the time interval; and S_{ult}=ultimate settlement. The values of ρ_0 and S_{ult} may be obtained through a regression analysis conducted on the t/S versus t relationship.

Ling et al. (1998) found that the hyperbolic function method provided a good prediction of long-term settlement in comparison with the logarithmic and the power function methods.

Comments on Different Methods

Park et al. (2002) evaluated the effects of waste decomposition on long-term settlement predictions for MSW landfills. They proposed separating long-term field compression behavior of MSW into two phases—the first dominated by mechanical processes of compression and the second dominated by decomposition. According to Park et al. (2002), the power creep method did not provide good predictions of long-term waste settlement. They noted that inclusion of accelerated logarithmic compression due to decomposition was necessary in order to successfully predict long-term settlement of MSW landfills.

Babu and Fox (1997) suggested that dividing settlements into primary and secondary components may not be realistic for landfills. They recommended evaluating total settlement behavior, while considering methods for landfill stabilization.

The rheological model, the power creep model, and the hyperbolic model do not require separation of settlement into primary and secondary components. However, these methods need further field verifications and, from a practical application point of view, are more involved than the Sowers method. At the present time, due to its simplicity and familiarity of consolidation based approach by practicing engineers, the Sowers method is widely used in the practice. This method has, therefore, been used to interpret the data from the case histories presented in this paper. It is likely that some of the other methods will gain acceptance in practice in the future, as additional documented case histories become available.

Time for Completion of Primary Settlement

Most of the initial refuse settlement, also called primary settlement, is due to physical and mechanical mechanisms. Secondary or long-term settlement, primarily due to physicochemical and biochemical decay, occurs under constant load after the completion of primary settlement. Primary settlement of municipal solid waste typically occurs within the first four months after load placement (Sowers 1973; Bjarngard and Edgers 1990; Sharma 2000; NAVFAC 1983). Thus, the value of t_1 in Eq. (3) can be between 1 and 4 months. In practice a value of 3–4 months is used for t_1 in Eqs. (7) and (8), as presented in the following. Settlement estimates for postclosure end use projects typically require calculations for ΔH_s made after about 15 to 20 years or longer following waste placement. In such cases, where t_2 is approximately say 20 years, the value of ΔH_s is not very sensitive to the choice of t_1 between three or 4 months.

Categories of Secondary Settlement

The secondary settlement, ΔH_s in a MSW landfill can be grouped into the following two categories, based on the type of loading applied:

1. Settlement under self-weight: This type of settlement is caused by the load imposed due to the weight of waste material on the underlying waste layers. The loading mechanism is different from an externally imposed load (such as either due to a structure or an earthen fill, discussed in the next section). The externally imposed load does not have a secondary settlement component due to its self weight. On the contrary, in the case of waste self-weight, the overlying waste material itself also undergoes settlement.

   As discussed earlier, the primary settlement of waste typically occurs during the first one to 4 months after waste placement. Thus, all of the primary settlement is generally over by the time a landfill is closed. The time required for primary settlement to complete depends on the nature of the material in the landfill. Some ground improvement techniques used to pretreat landfill waste material prior to construction over closed landfills tend to reduce the time required to complete primary settlement. This is discussed in further details later in this paper.

   For long-term settlement estimation, such as, for postclosure development, the time-dependent secondary settlement (ΔH_s), due to self-weight can be expressed by the following equation:

$$\Delta H_s = \Delta H_{(\text{SW})} = C_{\alpha(\text{SW})} H_1 \log \frac{t_2}{t_1} \tag{7}$$

   where $\Delta H_{(\text{SW})}$=settlement at time t_2 after fill placement; t_1=time for primary settlement, as discussed earlier; t_2=time of interest, since the self-weight was applied; H_1=thickness of refuse fill at the end of the primary settlement; and $C_{\alpha(\text{SW})}$=coefficient of secondary compression due to self-weight. Typical values for $C_{\alpha(\text{SW})}$ range between 0.1 and 0.4 (NAVFAC 1983).

J. Geotech. Geoenviron. Eng. 2007.133:619-629.

Technically Complete, March 11, 2016

Table 1. Summary of MSW C_{ce} and C_{α} Parameters from Literature

Reference	Primary C_{ce}	Secondary C_{α}
Sowers (1973)[a] (for e_0=3)	0.1–0.41 AVG = 0.25	0.02–0.07
Zoino (1974)[a]	0.15–0.33	0.013–0.03
Converse (1975)[a]	0.25–0.3	0.07
Rao et al. (1977)[a]	0.16–0.235	0.012–0.046
Oweis and Khera (1986)[a]	0.08–0.217	—
Landva et al. (1984)[a]	0.2–0.5	0.0005–0.029
Bjarngard and Edgers (1990)[a]	—	0.004–0.04
Wall and Zeiss (1995)[a]	0.21–0.25	0.033–0.056
Gabr and Valero (1995)[a]	0.2–0.23	0.015–0.023
Boutwell and Fiore (1995)[a]	0.09–0.19	0.006–0.012
Stulgis et al. (1995)[a]	0.16	0.02
Green and Jamenjad (1997)[a]	—	0.01–0.08
Landva et al. (2000)[a]	0.17–0.24	0.01–0.016
Zaminskie et al. (1994)	0.01–0.04	0.001–0.006
El-Fadel and Al-Rashed (1998)[b]	—	0.1–0.32 with leachate recirculation
Earth Tech (2001)[b]	—	0.18–0.26 with leachate recirculation
Park et al. (2002)	—	0.014–0.063 for "fresh waste"
		0.087–0.34 for waste undergoing active decomposition
Marques et al. (2003) (field monitoring)	0.073–0.132	—
Hossain et al. (2003) (laboratory testing)	0.16–0.37	0.015–0.03 for creep
		0.19 for waste undergoing active decomposition
Anderson et al. (2004) (field monitoring)	0.17–0.23	0.024–0.030
Calculated by authors Sharma (2000)	—	$C_{\alpha(\mathrm{EL})}$[c]: 0.02
		$C_{\alpha(\mathrm{SW})}$[d]: 0.19–0.28
Yolo County case history	—	$C_{\alpha(\mathrm{SW})}$: 0.04 for "fresh waste"
		$C_{\alpha(\mathrm{SW})}$: 0.16 for waste in bioreactor
Lewis et al. (2004) (field monitoring) for external load	—	$C_{\alpha(\mathrm{EL})}$:0.014 for waste treated with DDC[e]
	—	$C_{\alpha(\mathrm{EL})}$: 0.045 for waste treated with surcharge

[a]Data originally presented by Landva et al. (2000).
[b]Data originally presented by Hossain et al. (2003).
[c]EL=external load.
[d]SW=self-weight.
[e]DDC=deep dynamic compaction.

2. Settlement under external loads: After initial period of primary settlement (typically up to four months, as discussed previously) the time-dependent secondary settlement occurs over a long period of time in response to externally applied loads. This settlement can be expressed by the relationship similar to Eq. (7) and is presented as

$$\Delta H_s = \Delta H_{(\mathrm{EL})} = C_{\alpha(\mathrm{EL})} H_1 \log \frac{t_2}{t_1} \qquad (8)$$

where $\Delta H_{(\mathrm{EL})}$=settlement at time t_2 after external load application; t_1=time for primary settlement; t_2=time of interest, since the external load application; H_1=thickness of refuse fill at the end of the primary settlement; and $C_{\alpha(\mathrm{EL})}$=coefficient of secondary compression due to external loads.

Common examples of externally applied loads over landfills are final cover systems or construction of structures or fills. The intensity of external loads is typically much smaller than those due to self-weight of waste material in the landfill. Most external loads, especially those due to final cover system and/or structures, are typically applied only after the landfill has reached its final design grades and is ready for closure. Sometimes structures are constructed long after a landfill has been closed. Therefore, much of the self-weight settlement is completed by the time externally-applied loads are introduced. For this reason, since the amount of self-weight settlement during this period is very small, the writers do not consider it necessary to combine the calculations for self-weight and externally applied loads.

Literature review indicates that for older refuse fills which have undergone decomposition for some period of time (more than approximately 10 years), $C_{\alpha(\mathrm{EL})}$ ranges between 0.02 and 0.07 (NAVFAC 1983).

Both $C_{\alpha(\mathrm{SW})}$ and $C_{\alpha(\mathrm{EL})}$ values depend on site specific environmental conditions and waste composition, such as organic content of the waste fill. Higher compressibility, i.e., higher C_{α} values for both cases, will indicate higher organic content, higher humidity and/or higher degree of decomposition of the waste.

Typical Values for C_{ce} and C_{α}

Range of values for C_{ce} and C_{α} for MSW have been reported by various researchers. Landva et al. (2000) originally compiled a table presenting a summary of the range of values of C_{ce} and C_{α} reported in literature. Table 1 in this paper is a compilation of C_{ce} and C_{α} values from Landva et al. (2000) as well as from Anderson et al. 2004, Hossain et al. (2003), Marques et al. (2003), Park

J. Geotech. Geoenviron. Eng. 2007.133:619-629.

Technically Complete, March 11, 2016

Compression Indices for Full-Scale Landfills

Date: July 8, 2008

Completed by: Christopher Bareither

Compilation of primary and secondary compression indices from literature

Reference	Origin of Waste	Type of Waste[1]	Comments	Test Surface Area (m^2)	Surcharge Thickness (m)	Waste Thickness (m)	Average C_c'	Average C_α'
Andersen et al. (2004)	Everett Landfill, Washington State	MSW	Averages from extensometer data based on authors interpretation	—	8.64	5.54	0.2	0.027
Bachus et al. (2007)	Tennessee	MSW	Settlement plates on surface monitored for 6 months after construction of surface surcharge	42,100	3	18	0.33	0.010
								0.008
								0.008
								0.008
								0.010
								0.015
								0.007
								0.010
								0.020
			Settlement plates at various depths in landfill monitored for 6 months after construction of surface surcharge, waste thickness not reported	42,100	3	—		0.010
						—		0.008
						—		0.015
				10,525	6	—		0.019
						—		0.019
				4,210	9	—		0.025
						—		0.027
Boutwell & Flore (1994)	—	Filled early 1970s, left uncovered; MSW (Saturated)	Surcharge placed on unlined MSW/Industrial pit, settlement plates used to monitor surface settlement	100	1	5	0.09	0.007
				100	2	5	0.16	0.009
				100	3	5	0.19	0.012
Bowders and Mitchell (2005)	Columbia, Missouri	MSW - filled from 1986 - 1994	Settlement plate installed 7/23/1999; overburden constant for C_α' calc	—	1.2192	18	—	0.013
		MSW - filled from 1994 - 1998	Settlement plate installed 1/17/2002; overburden constant for C_α' calc	—	11	19	—	0.106
Coduto and Huitric (1990)	Spadra Landfill, Pomona, CA	MSW filled from 1976-1978	Monitored settlement at various depths in landfill with Sondex Tube; instruments installed May 1987, monitored through May 1989; report surface C_α' here	—	—	16	—	0.022
				—	—	22	—	0.021
Deutsch et al. (1994)	Honey Brook, PA (Lanchester)	MSW - newspapers readable to 1970s	—	—	—	9	0.22	—
Dodt et al. (1987)	Collier Road Landfill; Pontiac, MI	MSW and Industrial	Waste filled 1960's to 1985 (capped); 13 acre fill on top of landfill placed 1/1/1985 - 7/1/1986;	—	11	15	—	0.048
Sharma and De (2007)	Northern California	MSW ~ 15 years old	Dump since 1930's; sanitary landfill since 1969; 500,000 m3 fill places on toe of landfill; originally in Sharma et al. (1999)	—	—	16	—	0.020
	San Francisco Bay Area	Commercial	Filled 1956 - 1980s; compression under self weight of waste; originally in Sharma (2000)	—	—	6	—	0.220
	San Francisco Bay Area	Commercial	Filled 1956 - 1980s; compression under self weight of waste; originally in Sharma (2000)	—	—	36	—	0.190

	Southern California	Household and commercial	Filled 1976-1978; used sondex tubes - details in Coduto and Huitric (1990); originally in Sharma (2000)	—	—	16	—	0.280
	Southern California	Household and commercial	Filled 1976-1978; used sondex tubes - details in Coduto and Huitric (1990); originally in Sharma (2000)	—	—	23	—	0.270
Stulgis et al. (1995)	Massachusetts	All Types	Filled 1954 - 1985; ~ 30-50 yrs old in lowest 1/3 and 13-30 yrs old in upper 2/3	32	6.1	21	0.16	0.02
Watts and Charles (1990)	Brogborough (England) - filled 1983 - 1987	Domestic	Monitored settlement at various depths using magnetic extensometer; report active biodegradation during settlement monitoring	—	—	11	—	0.100
	Calvert (England) - filled 1979-1988			—	—	20	—	0.230
Yuen and Styles (2000)	Melbourne, Australia	Composition (dry mass basis) = 47% inert (C&D, soil, etc.), 12% paper, 9% plastic, 23% yard and food + some textile, metal and glass	Control Cell: 150 mm daily cover and 300 mm intermin cover every 2 m of waste (clayey sandy silt), approximately 15% of total volume	36,328	—	7	—	0.019
					—	13	—	0.041
					—	20	—	0.03
					—	43	—	0.028
Zamiskie et al. (1994)	Syosset landfill -- Oyster Bay, NY	C&D, minor MSW, ~ 66% soil	Operated from 1936-1976	—	2.75	17	0.03	0.0035

Summary statistics	Average C_c'	Average C_α'
Average	0.172	0.051
Maximum	0.330	0.280
Minimum	0.025	0.004
Coefficient of Variation	0.525	1.529

Reference No. 13

Interface Shear Strength Test Results
for Various Geosynthetic Interfaces

Technically Complete, March 11, 2016

Interface Friction Test Report

Client: **CB & I**
Project: **Rochelle Landfill, Final Cover Phase I**
Date: 07-22-2014 to 07-24-2014

TRI Log#: E2388-35-05
Test Method: ASTM D5321

John M. Allen, P.E., 07/24/2014
Quality Review/Date

Tested Interface: LPL-2 Soil vs. Skaps TN220-2-8 Double-sided Geocomposite (59971010001)

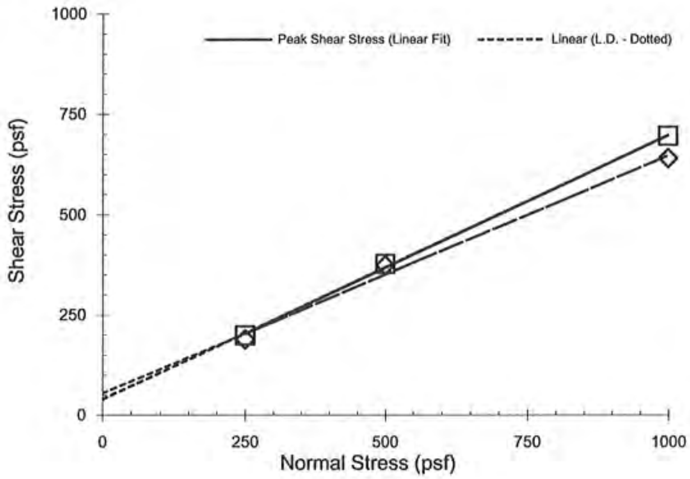

Test Results	Peak	Large Displacement (@ 3.0 in.)
Friction Angle (degrees):	33.4	30.7
Y-intercept or Adhesion (psf):	39	54

Shearing occurred at the interface.

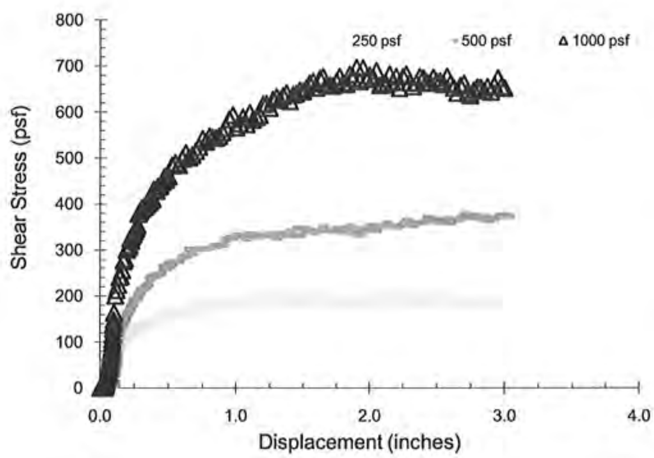

Test Conditions	
Upper Box &	LPL-2 Soil remolded to 109.0 pcf at 10.8% moisture content
Lower Box	Skaps TN220-2-8 double-sided geocomposite
Box Dimensions: 12"x12"x4"	
Interface Conditioning:	Interface soaked and loading applied for a minimum of 24 hours prior to shear.
Test Condition: Wet	
Shearing Rate: 0.04 inches/minute	

Test Data			
Specimen No.	1	2	3
Bearing Slide Resistance (lbs)	3	3	3
Normal Stress (psf)	250	500	1000
Corrected Peak Shear Stress (psf)	199	377	696
Corrected Large Displacement Shear Stress (psf)	188	373	640
Peak Secant Angle (degrees)	38.5	37.0	34.8
Large Displacement Secant Angle (degrees)	36.9	36.7	32.6
Asperity (mils)	--	--	--

Technically Complete, March 11, 2016

TRI/ENVIRONMENTAL, INC.

A Texas Research International Company

Interface Friction Test Report

Client: **Shaw Environmental**
Project: **Rochelle Landfill, Cell 1A & 2A**
Test Date: 08/24/12-08/30/12

TRI Log#: E2365-77-07
Test Method: ASTM D 5321

John M. Allen, P.E., 08/30/2012
Quality Review/Date

Tested Interface: CS-1 Soil vs. Agru 60 mil HDPE Microspike Geomembrane (443564.11)

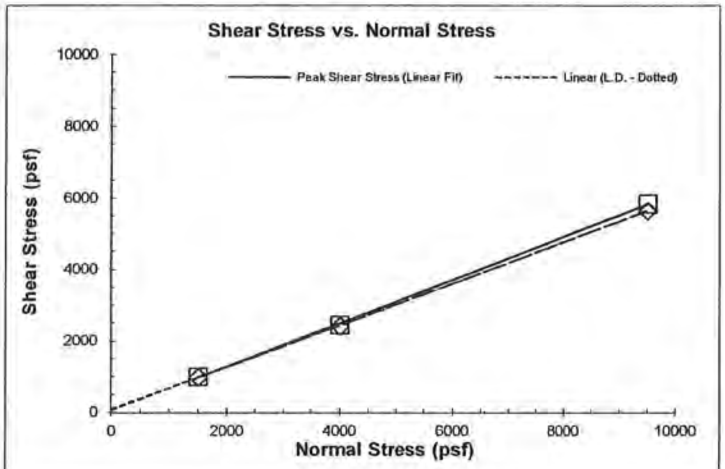

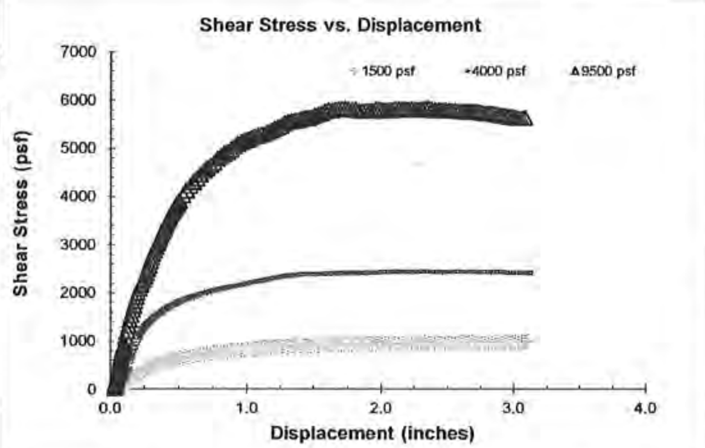

Test Results		
	Peak	**Large Displacement (@ 3.0 in.)**
Friction Angle (degrees):	**31.2**	**30.2**
Y-intercept or Adhesion (psf):	**65**	**104**

Shearing occurred at the interface.

Test Conditions

Upper Box & CS-1 Soil remolded to 125.7 pcf at 6.3% moisture content

Lower Box Agru 60 mil HDPE Microspike geomembrane (shiny side)

Box Dimensions: 12"x12"x4"

Interface Conditioning: Interface loading applied for a minimum of 24 hours prior to shear.

Test Condition: Wet

Shearing Rate: 0.04 inches/minute

Test Data

Specimen No.	1	2	3
Bearing Slide Resistance (lbs)	22	46	98
Normal Stress (psf)	1500	4000	9500
Corrected Peak Shear Stress (psf)	999	2456	5839
Corrected Large Displacement Shear Stress (psf)	987	2421	5642
Peak Secant Angle (degrees)	33.7	31.5	31.6
Large Displacement Secant Angle (degrees)	33.3	31.2	30.7
Asperity (mils)	35.0	37.4	37.4

9063 Bee Caves Road □ Austin, TX 78733-6201 □ (512) 263-2101 □ (512) 263-2558 □ 1-800-880-TEST

TRI/ENVIRONMENTAL, INC.
A Texas Research International Company

Interface Friction Test Report

Client: **Veolia**
Project: **Zion, Site 2 Expansion, Cell 5B**
Test Date: 07/31/07-08/02/07

TRI Log#: E2279-28-08
Test Method: ASTM D 5321

John M. Allen, E.I.T., 08/02/2007
Quality Review/Date

Tested Interface: Clay Soil (ZL-CS-1) vs. GSE 60 mil HDPE Textured Geomembrane (105134664)

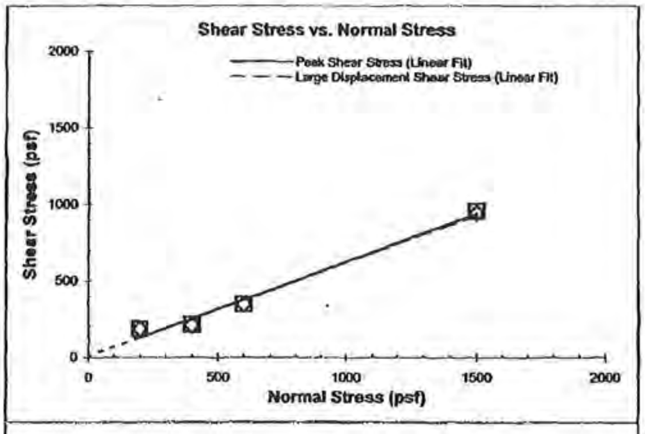

Test Results		
	Peak	Large Displacement (@ 3.0 in.)
Friction Angle (degrees):	31.9	31.5
Y-Intercept or Adhesion (psf):	6	8

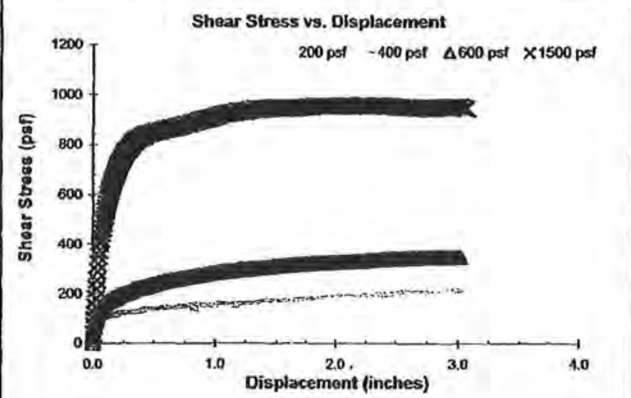

Test Conditions

Upper Box & Clay soil (ZL-CS-1) remolded to 116.9 pcf at 9.1%

Lower Box GSE 60 mil HDPE textured geomembrane

Box Dimensions: 12"x12"x4"

Interface Conditioning: Interface soaked and loading applied for a minimum of 24 hours prior to shear.

Test Condition: Wet

Shearing Rate: 0.04 inches/minute

Test Data

Specimen No.	1	2	3	4
Bearing Slide Resistance (lbs)	10	12	14	22
Normal Stress (psf)	200	400	600	1500
Corrected Peak Shear Stress (psf)	186	215	347	956
Corrected Large Displacement Shear Stress (psf)	186	213	347	944
Peak Secant Angle (degrees)	42.9	28.3	30.1	32.5
Large Displacement Secant Angle (degrees)	42.9	28.0	30.0	32.2
Asperity (mils)	17.8	16.0	16.8	17.0

9063 Bee Caves Road □ Austin, TX 78733-6201 □ (512) 263-2101 □ (512) 263-2558 □ 1-800-880-TEST

Technically Complete, March 11, 2016

TRI/ENVIRONMENTAL, INC.

A Texas Research International Company

Interface Friction Test Report

Client: **Veolia**
Project: **Zion, Site 2 Expansion, Cell 5B**
Test Date: 07/31/07-08/02/07

TRI Log#: E2279-28-08
Test Method: ASTM D 5321

John M. Allen, E.I.T., 08/02/2007
Quality Review/Date

Tested Interface: Clay Soil (ZL-CS-1) vs. GSE 60 mil HDPE Textured Geomembrane (105134664)

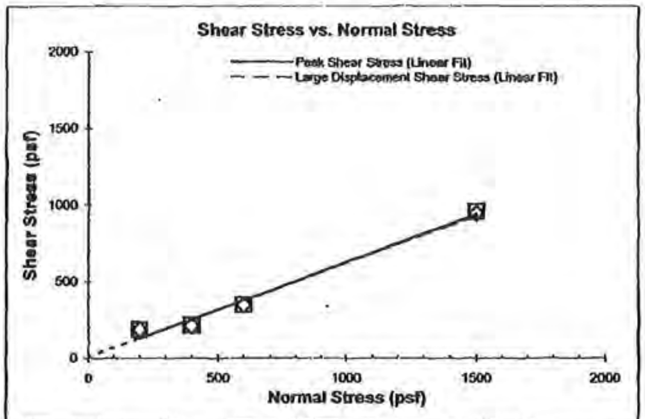

Test Results

	Peak	Large Displacement (@ 3.0 in.)
Friction Angle (degrees):	**31.9**	**31.5**
Y-Intercept or Adhesion (psf):	**6**	**8**

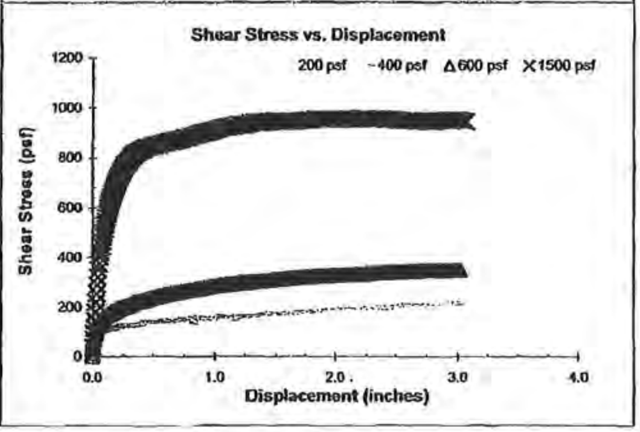

Test Conditions

Upper Box &	Clay soil (ZL-CS-1) remolded to 116.9 pcf at 9.1%
Lower Box	GSE 60 mil HDPE textured geomembrane
Box Dimensions: 12"x12"x4"	
Interface Conditioning:	Interface soaked and loading applied for a minimum of 24 hours prior to shear.
Test Condition: Wet	
Shearing Rate: 0.04 inches/minute	

Test Data

Specimen No.	1	2	3	4
Bearing Slide Resistance (lbs)	10	12	14	22
Normal Stress (psf)	200	400	600	1500
Corrected Peak Shear Stress (psf)	186	215	347	956
Corrected Large Displacement Shear Stress (psf)	186	213	347	944
Peak Secant Angle (degrees)	42.9	28.3	30.1	32.5
Large Displacement Secant Angle (degrees)	42.9	28.0	30.0	32.2
Asperity (mils)	17.8	16.0	16.8	17.0

9063 Bee Caves Road □ Austin, TX 78733-6201 □ (512) 263-2101 □ (512) 263-2558 □ 1-800-880-TEST

Technically Complete, March 11, 2016

TRI/ENVIRONMENTAL, INC.
A Texas Research International Company

Interface Friction Test Report

Client: **Shaw Environmental**
Project: **Rochelle Landfill, Cell 1A & 2A**
Test Date: 08/24/12-08/30/12

TRI Log#: E2365-77-07
Test Method: ASTM D 5321

John M. Allen, P.E., 08/30/2012
Quality Review/Date

Tested Interface: CS-1 Soil vs. Agru 60 mil HDPE Microspike Geomembrane (443564.11)

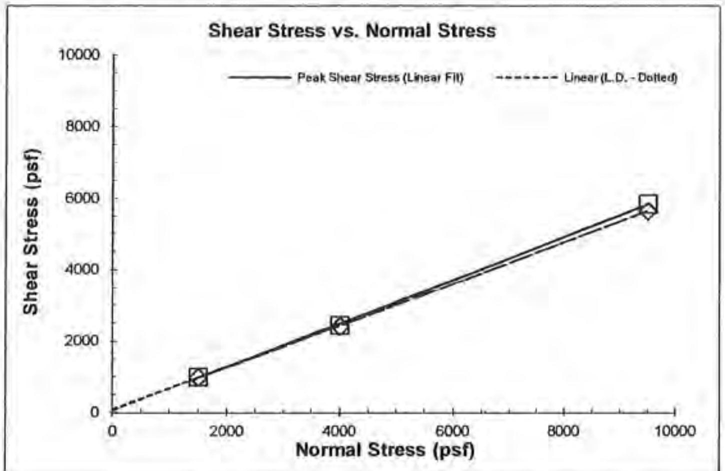

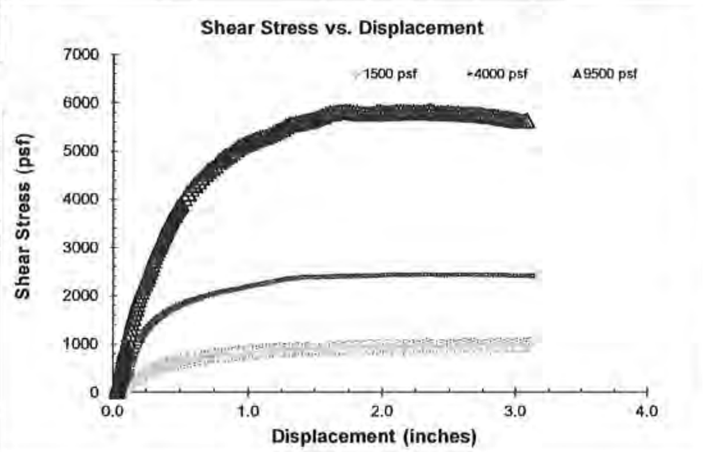

Test Results	Peak	Large Displacement (@ 3.0 in.)
Friction Angle (degrees):	31.2	30.2
Y-intercept or Adhesion (psf):	65	104

Shearing occurred at the interface.

Test Conditions

Upper Box & CS-1 Soil remolded to 125.7 pcf at 6.3% moisture content

Lower Box Agru 60 mil HDPE Microspike geomembrane (shiny side)

Box Dimensions: 12"x12"x4"

Interface Conditioning: Interface loading applied for a minimum of 24 hours prior to shear.

Test Condition: Wet

Shearing Rate: 0.04 inches/minute

Test Data

Specimen No.	1	2	3
Bearing Slide Resistance (lbs)	22	46	98
Normal Stress (psf)	1500	4000	9500
Corrected Peak Shear Stress (psf)	999	2456	5839
Corrected Large Displacement Shear Stress (psf)	987	2421	5642
Peak Secant Angle (degrees)	33.7	31.5	31.6
Large Displacement Secant Angle (degrees)	33.3	31.2	30.7
Asperity (mils)	35.0	37.4	37.4

9063 Bee Caves Road □ Austin, TX 78733-6201 □ (512) 263-2101 □ (512) 263-2558 □ 1-800-880-TEST

Reference No. 14

USGS Seismic Hazard Map of the U.S.

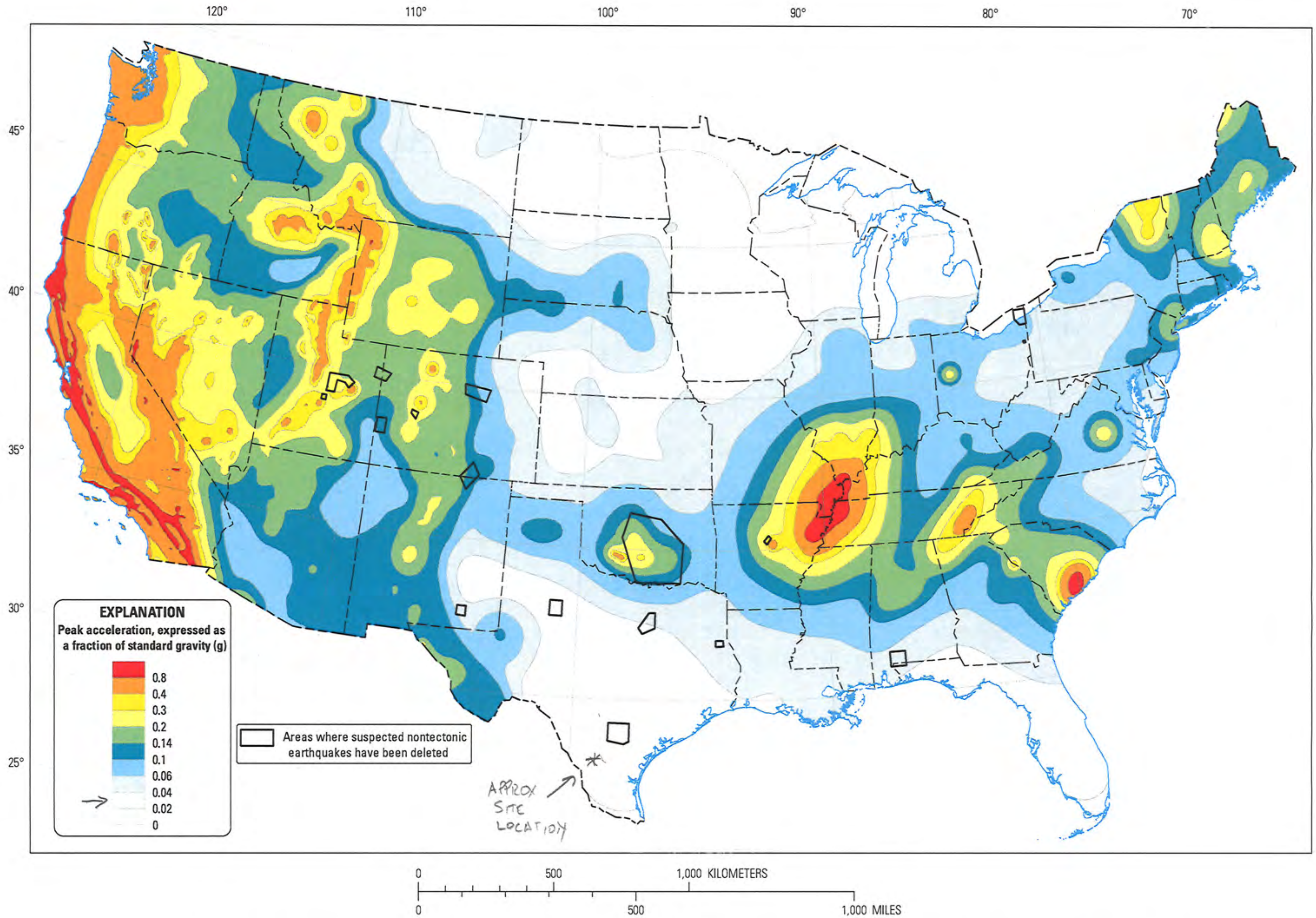

Two-percent probability of exceedance in 50 years map of peak ground acceleration

Source: The U.S. Geological Survey (USGS) - 2014 National Seismic Hazard Map

Reference No. 15

USEPA - Solid Waste Disposal Facility
Criteria Technical Manual
(*Recommended Safety Factors*)

Technically Complete, March 11, 2016

United States Environmental Protection Agency | Solid Waste and Emergency Response (5305) | EPA530-R-93-017 November 1993 www.epa.gov/osw

EPA

Solid Waste Disposal Facility Criteria

Technical Manual

TABLE OF CONTENTS

Principal modes of failure in soil or rock include:

- Rotation (change of orientation) of an earthen mass on a curved slip surface approximated by a circular arc;
- Translation (change of position) of an earthen mass on a planar surface whose length is large compared to depth below ground;
- Displacement of a wedge-shaped mass along one or more planes of weakness;
- Earth and mud flows in loose clayey and silty soils; and
- Debris flows in coarse-grained soils.

For the purposes of this discussion, three types of failures can occur at a landfill unit: settlement, loss of bearing strength, and sinkhole collapse.

- If not properly engineered, a landfill in an unstable area may undergo extreme **settlement**, which can result in structural failure. Differential settlement is a particular mode of failure that generally occurs beneath a landfill in response to consolidation and dewatering of the foundation soils during and following waste loading.

  Settlement beneath a landfill unit, both total and differential, should be assessed and compared to the elongation strength and flexure properties of the liner and leachate collection pipe system. Even small amounts of settlement can seriously damage leachate collection piping and sumps. The analysis will provide an estimate of maximum settlement, which can be used to aid in estimating differential settlement.

  Allowable settlement is typically expressed as a function of total settlement because differential settlement is more difficult to predict. However, differential settlement is a more serious threat to the integrity of the structure than total settlement. Differential settlement also is discussed in Section 6.3 of Chapter 6.

- **Loss of bearing strength** is a failure mode that tends to occur in areas that have soils that tend to expand, rapidly settle, or liquefy, thereby causing failure or reducing performance of overlying MSWLF components. Another example of loss of bearing strength involves failures that have occurred at operating sites where excavations for landfill expansions adjacent to the filled areas reduced the mass of the soil at the toe of the slope, thereby reducing the overall strength (resisting force) of the foundation soil.

- **Catastrophic collapse in the form of sinkholes** is a type of failure that occurs in karst regions. As water, especially acidic water, percolates through limestone (calcium carbonate), the soluble carbonate material dissolves, forming cavities and caverns. Land overlying caverns can collapse suddenly, resulting in sinkhole features that can be 100 feet or more in depth and 300 feet or more in width.

Tables 2-2 and 2-3 provide examples of analytical considerations for mode of failure assessments in both natural and human-made slopes.

Table 2-4

Recommended Minimum Values of Factor of Safety for Slope Stability Analyses

	Uncertainty of Strength Measurements	
Consequences of Slope Failure	Small[1]	Large[2]
No imminent danger to human life or major environmental impact if slope fails	1.25 (1.2)*	1.5 (1.3)
Imminent danger to human life or major environmental impact if slope fails	1.5 (1.3)	2.0 or greater (1.7 or greater)

[1] The uncertainty of the strength measurements is smallest when the soil conditions are uniform and high quality strength test data provide a consistent, complete, and logical picture of the strength characteristics.

[2] The uncertainty of the strength measurements is greatest when the soil conditions are complex and when available strength data do not provide a consistent, complete, and logical picture of the strength characteristics.

* Numbers without parentheses apply for static conditions and those within parentheses apply to seismic conditions.

Source: EPA Guide to Technical Resources for the Design of Land Disposal Facilities.